JAEA-Technology
2009-046

Analytical Study of Cover Plate Welding Deformation of the Radial Plate of the ITER Toroidal Field Coil

Junji OHMORI, Norikiyo KOIZUMI, Tatsuya SHIMIZU
Kiyoshi OKUNO and Mitsuru HASEGAWA

Division of ITER Project
Fusion Research and Development Directorate

September 2009
Japan Atomic Energy Agency
日本原子力研究開発機構

JAEA-Technology

JAEA-Technology 2009-046

Analytical Study of Cover Plate Welding Deformation of the Radial Plate of the ITER Toroidal Field Coil

Junji OHMORI, Norikiyo KOIZUMI, Tatsuya SHIMIZU※,
Kiyoshi OKUNO and Mitsuru HASEGAWA*

Division of ITER Project
Fusion Research and Development Directorate
Japan Atomic Energy Agency
Naka-shi, Ibaraki-ken

(Received July 7, 2009)

The winding pack (WP) of the Toroidal Field (TF) coil of ITER consists of 7 double-pancakes (DPs). In the DP, the conductor is embedded in a groove of a radial plate (RP), and cover plates (CP) are welded to the RP teeth to fix the conductors in the RP groove. The dimensions of the DP are 15 m in height and 9 m in width while the tolerances of the DP are very severe, such as a flatness of 2mm and an in-plane deviation of a few millimeters. It is therefore required to reduce the deformation of the DP by CP welding. In order to estimate welding deformation, the authors apply an analytical method in which the CP welding deformation of the DP can be calculated using inherent strain evaluated from welding deformation measured using a RP mock-up. Calculated results indicate that out-of-plane distortion can be kept to within required tolerances, but in-plane deformation is larger than allowed when welding thickness is 2.5 mm. The in-plane deformation is mainly caused by the bending of the curved RP region. Therefore, reducing the welding thickness at the curved region emerges as the most promising solution of this issue. Calculated results assuming a welding thickness of 1 mm at the curved region show that the in-plane deformation conforms to required tolerances. Furthermore, since the maximum out-of-plane deformation is within tolerances but marginal, an alternative design in which the number of welding lines is half that of the reference design, is proposed not only to improve the out-of-plane distortion but also to simplify the manufacture of the DP. It is found that the alternative design is effective in reducing welding distortion.

Keywords: ITER, TF Coil, Cover Plate, Welding Deformation

※ Collaborating Engineer
＊ Mitsubishi Electric Corporation

ITER トロイダルコイルのカバープレートの溶接変形検討と設計提案

日本原子力研究開発機構
核融合研究開発部門　ITER プロジェクトユニット

大森　順次、小泉　徳潔、清水　辰也※、
奥野　清、長谷川　満*

（2009 年 7 月 7 受理）

ITER のトロイダル磁場(TF)コイルの巻線は、7 ダブル・パンケーキ（DP）で構成される。DP では、導体はラジアル・プレート(RP)の溝に埋め込まれ、導体を RP の溝に収めた後、カバー･プレート(CP)を RP に溶接して導体を固定する。RP の大きさは、高さ 15 m、幅 9 m であるのに対して、その製作公差は平面度で 2 mm、面内変形で約 2.5 mm と極めて厳しい。そのため、CP 溶接による RP の変形を極力小さくする必要がある。この変形を予測するために、モック・アップ RP の CP 溶接試験の溶接変形の測定結果から得られた固有歪を用いて、DP の CP 溶接変形を解析した。この解析結果から、面外変形は要求される許容値以内にすることが可能だが、面内変形は溶接深さが 2.5 mm の場合は許容値を超えることが分かった。面内変形は主に RP 曲線部の曲げによって生じる。それ故、アウト・ボードでの溶接深さを減少させることはこの問題の解決策として有効と考えられる。アウト･ボードでの溶接深さを 1mm とした解析では、面内変形は許容値内となった。さらに、面外の最大変形は許容値内ではあるが、許容限界に近いので、面外変形の改善のみだけでなく DP の製作を単純化できる代替構造を提案した。代替構造では、溶接線が現設計の半分となり、特に、面外溶接変形を減少させることができることが分かった。

那珂核融合研究所(駐在)：〒311-0193　茨城県那珂市向山 801-1
※ 技術開発協力員
＊ 三菱電機株式会社

Contents

目　　次

1. Introduction

The ITER Toroidal Field (TF) Coil [1] has a D-shaped winding pack （WP） contained in a thick stainless steel case. The WP consists of seven double pancakes (DPs), each of which is designed to have a radial plate (RP) to enhance the mechanical and electrical reliability of the electrical insulation. The RP has grooves on both surfaces in which the conductor is placed. The conductor is fixed in the groove by welding the cover plates (CP) to the RP teeth.

Although the total length of all welds for each regular DP measures approximately 1.5 km, the required flatness is 2 mm and the tolerance of in-plane deviation from the current center line (CCL) is 2 mm at the inboard, and 3 mm at the outboard, respectively. These levels of deviation from the CCL represent tolerances of approximately ±2.5 mm of in-plane displacement. Since 1-mm deviation of the flatness is assumed in the RP manufacture itself, the allowable tolerance of the flatness for the CP welding is 1 mm. These severe tolerances for the RP represent one of the main issues in the fabrication of the WP.

However, welding deformation of a RP is difficult to extrapolate from test results of sub-size RP models. Of course, deformation may be evaluated through manufacturing a dummy DP. Due to high manufacturing costs, we cannot afford to fail in the manufacture of a dummy DP and, in addition, efforts should be made beforehand to increase the likelihood of success of any demonstration. We are therefore interested in estimating the deformation of a real RP before manufacturing a dummy DP. One possible solution of this requirement is thermal elastoplastic analysis, taking into account details of local welding deformation and thermal behavior. However, it takes quite a long time and then may be difficult to apply this method to a full scale RP. The authors thus proposed applying a simpler analytical method in which CP welding deformation of the DP can be calculated using inherent strain [2] evaluated from CP welding deformation of a RP mock-up. Note that applicability of this method is demonstrated at present only on a small scale, but it represents a promising approach to predicting CP welding deformation of a real RP, in part because we have few feasible alternatives.

In this report, details of the RP and CP are first explained. Secondly, results of the CP welding test for a 1-m RP mock-up on an inboard curved region are briefly interpreted, and the details of the simulation are described. Furthermore, the simulation results of CP welding deformation using an alternative design, proposed by the authors so as to reduce welding deformation and simplify the manufacturing procedure, are reported.

2. Radial plate (RP) and cover plate (CP)

Seven DPs, namely five regular RPs and two side RPs, are stacked together to form the WP, as shown in **Fig.2-1**. The height, the width and the thickness of the WP are 14.7 m, 8.7 m and 0.83 m, respectively, as shown in **Fig.2-2**. A TF conductor wound with glass-polyimide multilayer tape is placed in a groove on each surface of a RP. The cross sections of regular and side DPs are shown in **Fig.2-3**. **Figure 2-4** shows a cross section of the regular RP. Since the winding dimension has some error during winding and changes following heat treatment [3], some gap between the conductor and the RP teeth is necessary to avoid damaging conductor performance and the insulation layers as a result of applying strain to the conductor while inserting the conductor into the RP groove. However, since the expected force on the RP is high and low at the inboard and outboard, respectively, the gap is minimized at the inboard and becomes wider at the outboard. In addition, since the DP is higher than it is wide, the gap between the conductor and the RP teeth is wider at the top and bottom than at the outboard. Thus, the cross sections of the RP are slightly different along the inboard, outboard, top and bottom.

Figure 2-5 shows the dimensions of the CP and the RP. The cross section of the CP is also different depending on the width of the RP groove. CPs are welded to a RP tooth through laser welding after insertion of the conductor with the insulation layers into the RP groove. The welding thickness is 2 mm in the reference design.

The tolerances for the RP are described in the previous section and shown in Figs.2-2 and 2-3.

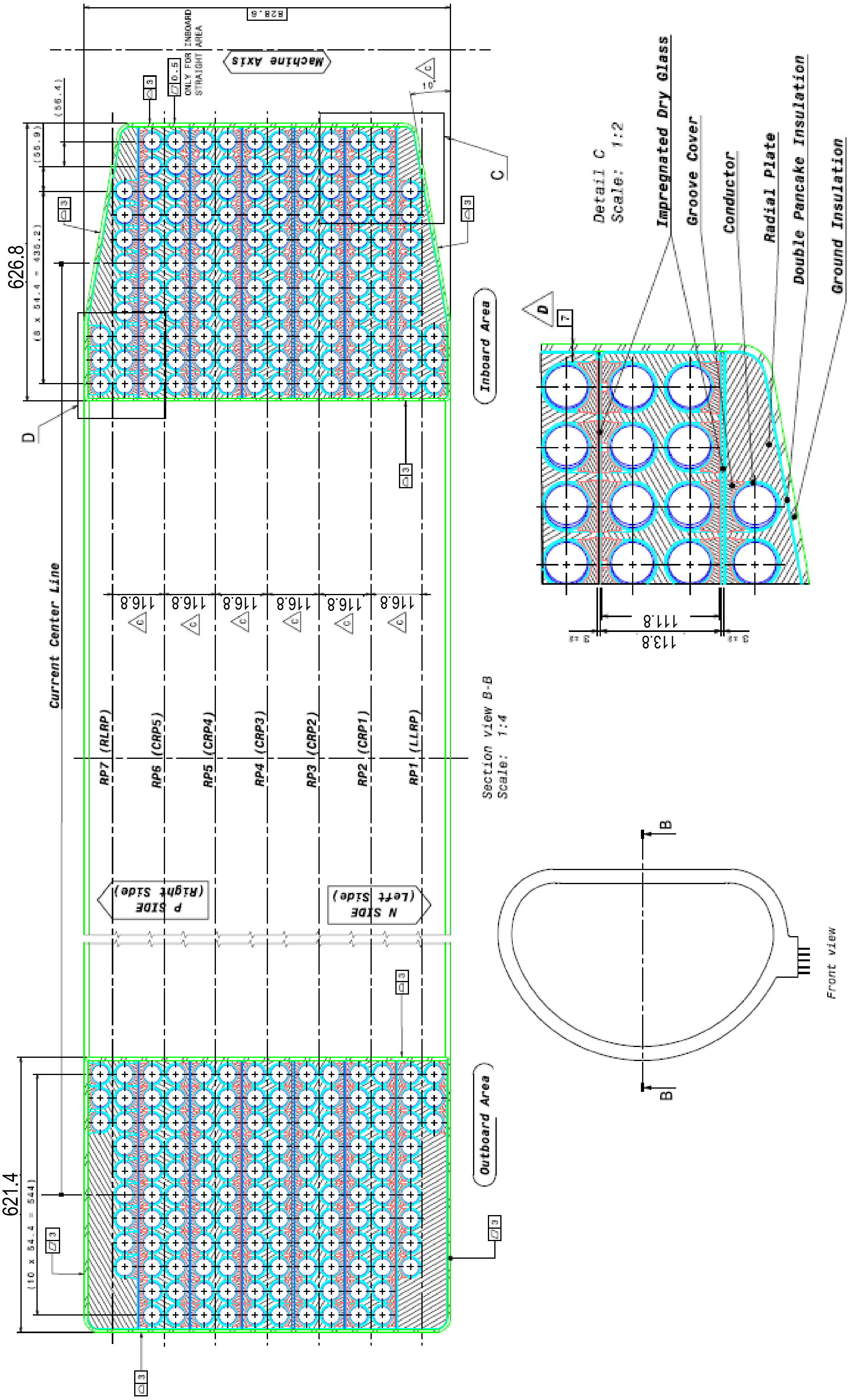

Fig2-1 Cross section of TF coil winding pack (WP)

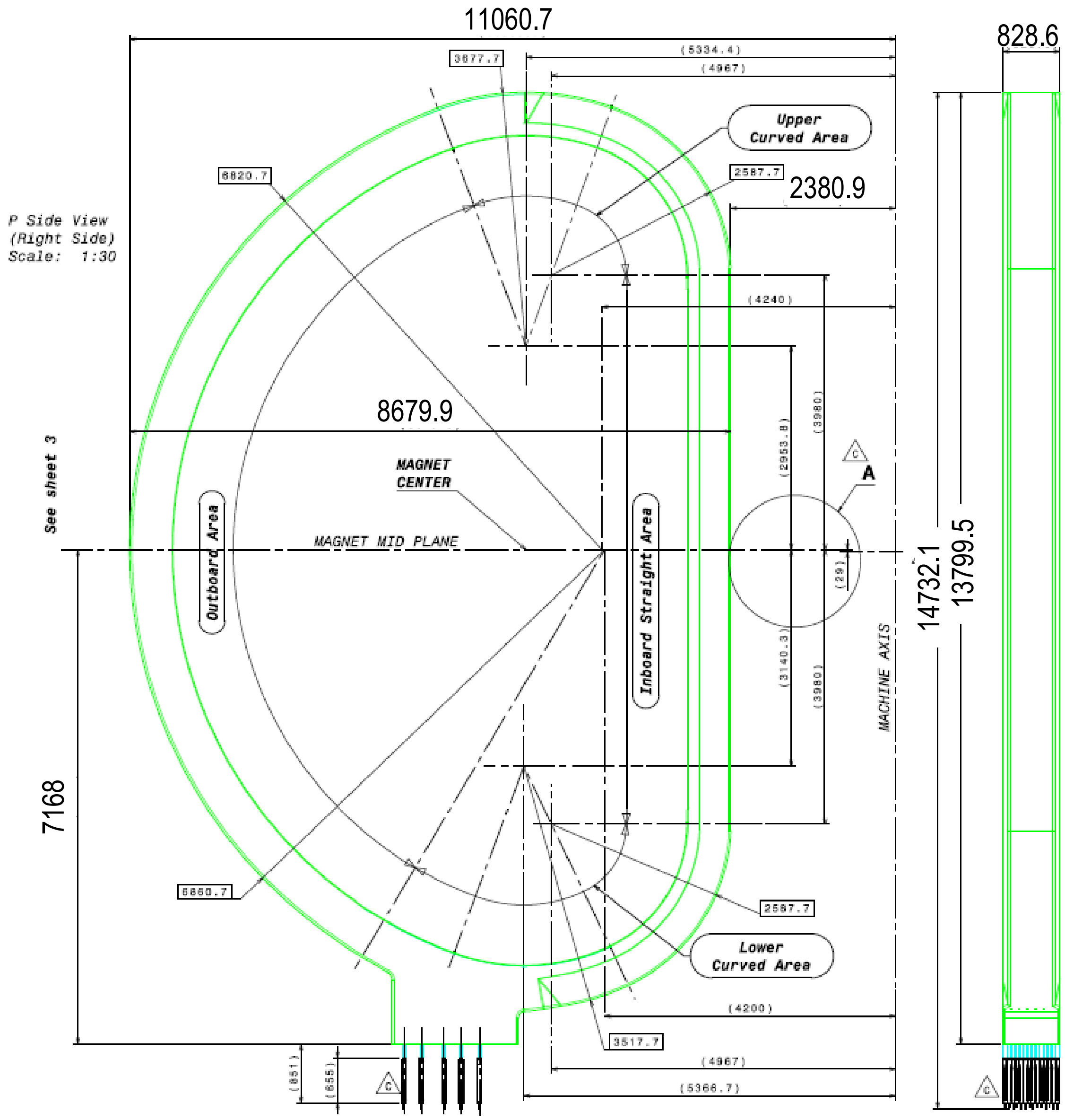

Fig2-2 Dimensions of the TF coil winding pack (WP)

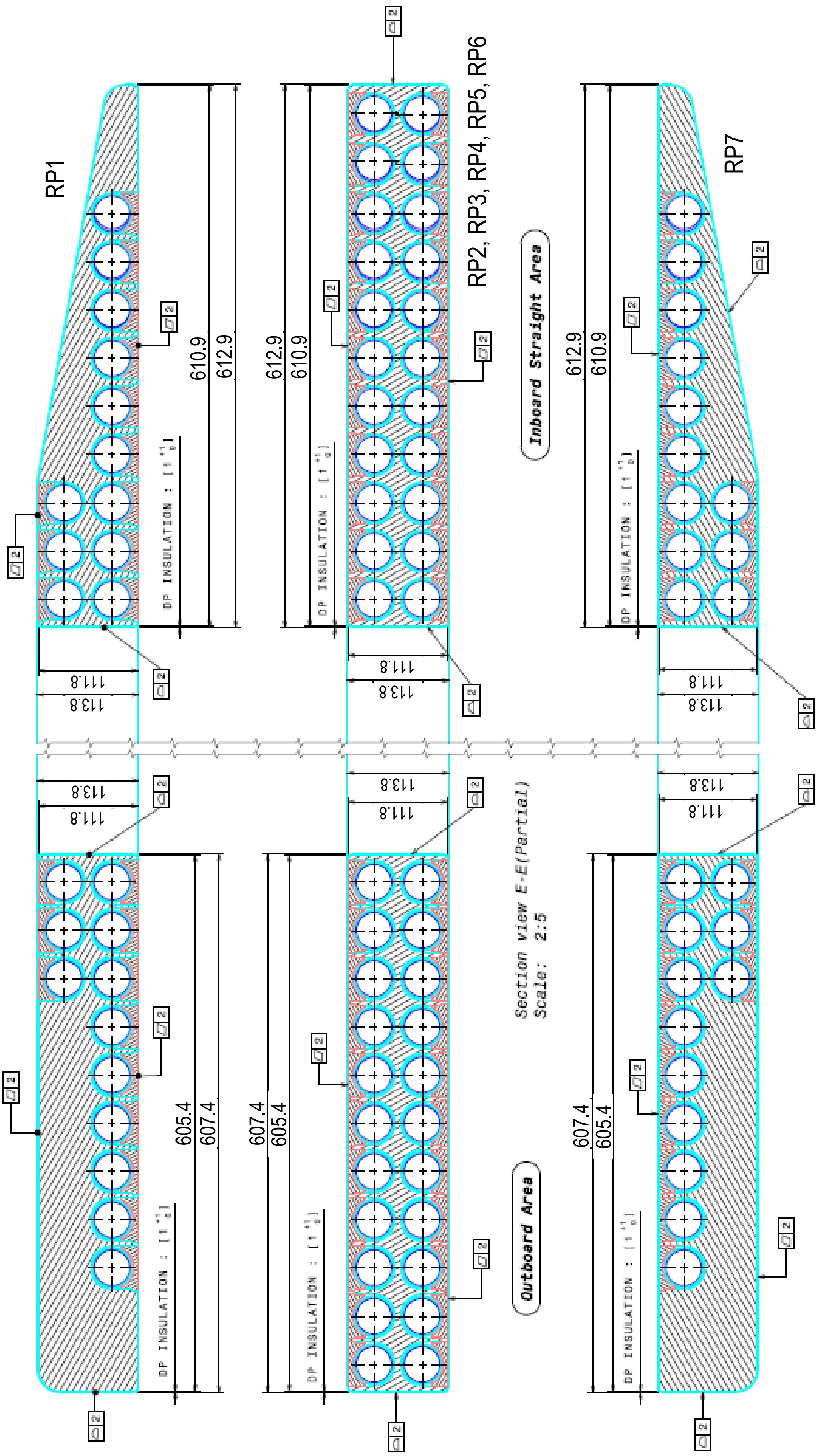

Fig2-3 Cross section of a radial plate (RP)

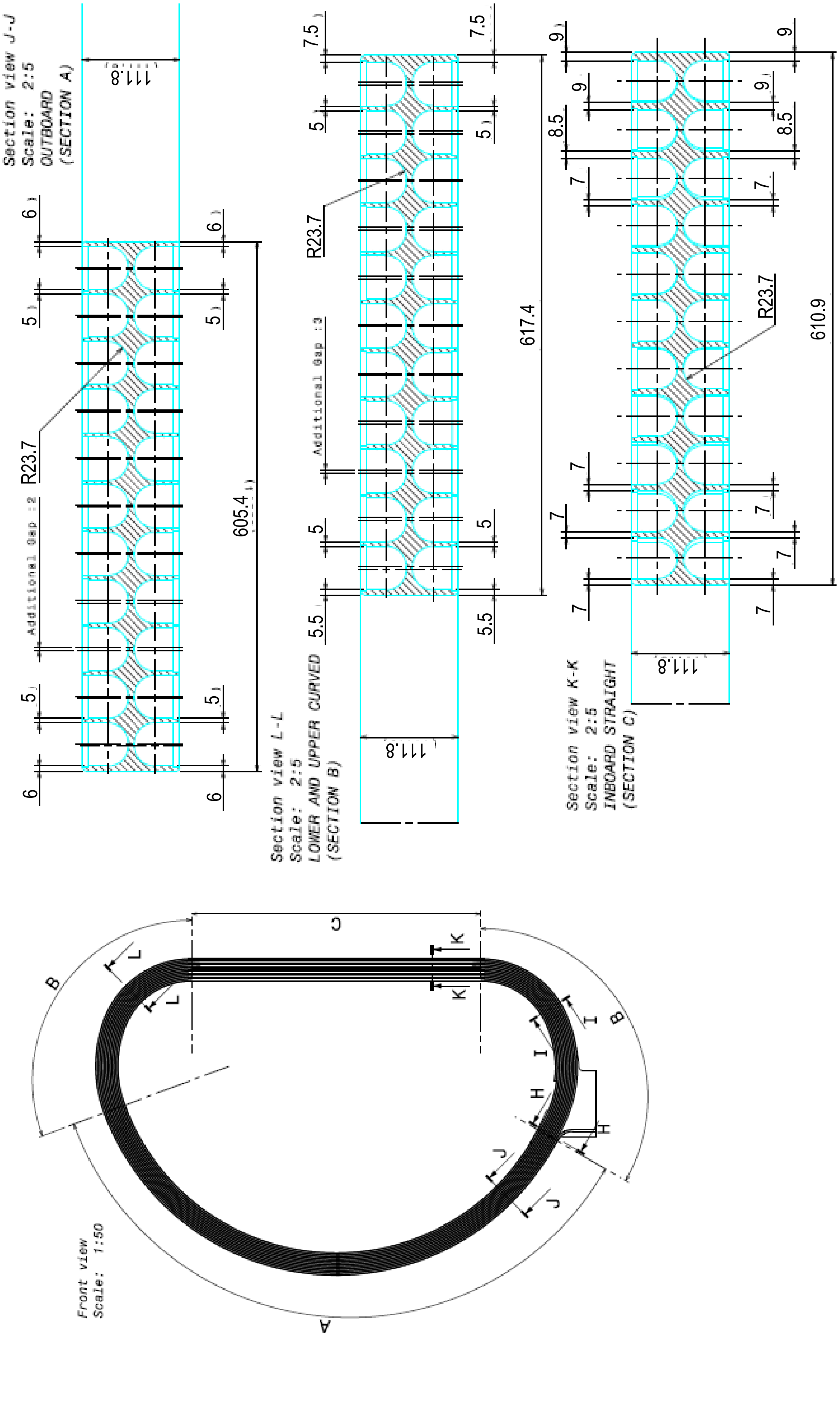

Fig2-4 Cross section of a regular radial plate (RP)

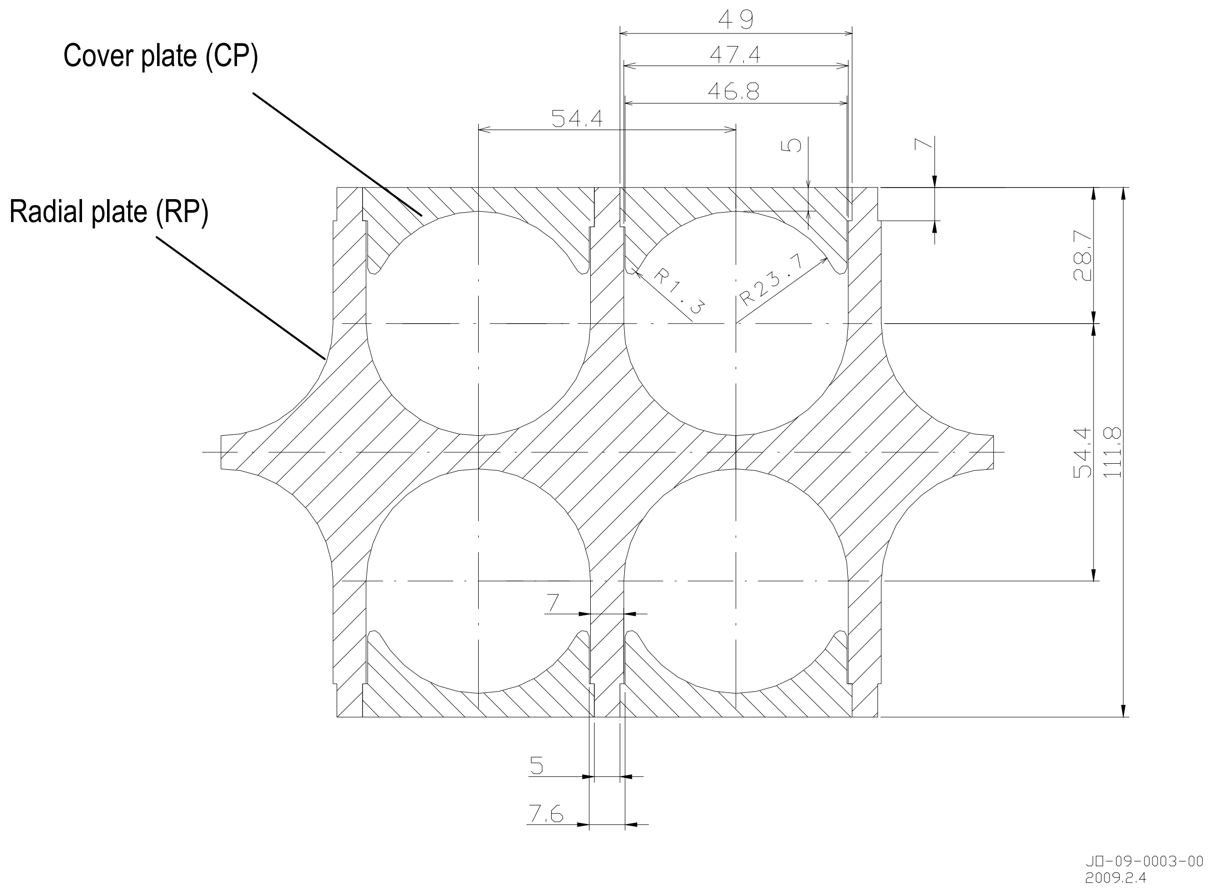

Fig 2-5 Typical dimensions of a cover plate (CP) and a radial plate (RP)

3. CP welding test using a curved inboard RP mock-up

3.1 Test method

The sample used in the CP welding test is part of the inboard curved region with a Poloidal angle of 22 degrees and length of about 1m. Since it was fabricated a few years ago, the cross-sectional dimension is that of the previous design, which is slightly different from the reference design. The dimensions of the RP mock-up and the CP are shown in **Figs.3.1-1** and **3.1-2**. The RP mock-up and CPs are made of SS316LN and SS316L.

The welding conditions are as follows;

3.1.1 Welding parameters

1) YAG laser
   - Power: 2 kW (target welding thickness of 2.5 mm with a margin of 0.5 mm from the designed welding thickness of 2 mm)
   - Diameter of fiber: ϕ0.6 mm
   - Diameter of laser spot: ϕ0.6 mm
   - Focus: f=200 mm
   - Sealed gas: N_2 (40 l/min)
2) Welding speed: 2 m/min
3) Other conditions
   - Position of the RP mock-up: horizontal
   - Number of weld lines at one time: one line
   - Allowable maximum gap between the CPs and RP teeth: less than 0.2 mm (if a gap was wider than 0.2 mm, shims were inserted to keep the width of the gap less than 0.2 mm)
   - Laser tack- welding: welding pitch of 100 mm in the circumferential direction
     Laser power: 1.5 kw
     Head speed 2 m/min
     Duration: 0.2 sec (bead length: 7 mm)
4) Sequence of welding
   - Welding 22 lines on the first plane (P side), and then welding 22 lines on the other plane (N side).
   - The CP welding started in the middle of the RP, and the adjacent inner and outer CPs on the P side were alternatively welded, as shown in **Fig.3.1-3**. This sequence was determined from a preliminary analysis of inherent strain to minimize out-of-plane distortion. It is, for example, indicated that a weld

sequence, starting from the innermost point and moving outward, produces a 20% larger out-of-plane distortion compared to the above.

Figure 3.1-4 shows the welding machine.

3.1.2 Restraint of RP mock-up

Deformation due to welding may be reduced by fixing the RP mock-up to robust beams along the upper and lower surfaces of the RP. However, if such restraints are used, laser welding must be conducted twice to weld the area covered by the beam at the outset. Since shifting the restraint could be time consuming during the CP welding of the TF coil DP, the RP mock-up was fixed to a support beam only at the inner and outer surfaces to omit the need to shift the support beam, as shown in **Fig. 3.1-5**.

3.1.3 CP welding and filling the gap between the CP and RP teeth

Due to the difficulty of machining all CPs to a high degree of accuracy so as to achieve a gap narrower than 0.2 mm between the CP and the RP teeth, some shims were inserted into the gaps on both surfaces of the RP mock-up to enable laser welding, as in the case of the TFMC. The CP was then tack-welded by TIG welding at three points along each welding line on both surfaces of the RP mock-up. These preparations enabled laser tack-welding to be performed every 100 mm on the P side. All welding lines on the P side subsequently were welded. The same procedure was repeated on the N side.

The gaps between the CP and the RP teeth on the N side were expanded by laser welding on the P side. These gaps could not be reduced as a result of fixing only the inner and outer surfaces of the RP mock-up when the RP mock-up was turned upside down. Consequently, after laser welding on the P side, shims were added to fill those gaps on the N side which had become too big to laser-weld.

3.1.4 Measuring the deformation

Points where the welding deformation was measured are as follows and shown in **Fig.3.1-6**.

- Flatness of the RP mock-up: 36 points / surface (SP1 - SP6 and SN1 - SN36)
- Dimensions in the circumferential direction: 9 points (LP1 - LP3, LC1 - LC3 and LN1 - LN3).
- Dimensions in the radial direction: 9 points (WP1 - WP3, WC1 - WC3 and WN1 - WN3).

- Flatness of the CP: 3 points / surface (CP1 - CP3 and CN1 - CN3). Measured points are in the center of the width of the CP.

3.2 Results

3.2.1 Gap filling

Figures 3.2-1 shows locations where shims were inserted. The shims were 0.1 and 0.2 mm thin plates or a combination thereof. **Figure 3.2-2** shows the gaps with inserted shims.

3.2.2 CP welding

Figures 3.2-3 and **3.2-4** show the laser tack-welded RP mock-up and a laser tack-welding bead, respectively. After the laser tack-welding, the CP welding on all welding lines was performed as may be seen in **Fig.3.2-5**. Undercutting of the welding bead was observed after CP welding. **Figures 3.2-6** and **3.2-7** indicate the locations of the undercutting of the welding bead on the P and N sides, respectively. **Figure 3.2-8** shows a typical undercut. Where there was a gap of more than 0.15 mm, an undercut occurred, especially on the N side.

Since a large gap between the CP and RP teeth was observed and filled with shims, as mentioned above, the welding thickness for such a wide gap was investigated using a small specimen. **Figure 3.2-9** shows a cross-sectional view of the specimen with 4 shims, each with a thickness of 0.2 mm. The maximum gap in the CP welding test, 0.8 mm, was simulated in this specimen. Although the weld surface looks good, the effective welding thickness in which the weld metal is completely melted, is 1.1 mm, which is less than half of the target welding thickness of 2.5 mm. Therefore, there is a possibility that the welding thickness is thinner than the target of 2.5 mm at points with a wide gap.

3.2.3 Out-of-plane distortion

Figures 3.2-10 -12 show the measured out-of-plane distortion, defined as a change in dimensions due to the CP welding. The distortions are measured against a baseline adjustment in which the vertical coordinate of a line connecting the innermost and outermost surfaces of the RP mockup is zero at θ=0. The temperature at the time of measurement was 17 - 19 °C.

The out-of-plane distortion of CPs is shown in **Fig.3.2-13**. CP1 - CP3 denote the measured locations on the CPs. The center of the width of the CP was elevated by 0.1mm from the RP surface.

The results for out-of-plane distortion are summarized in **Table 3.2-1**. The maximum distortion is 1.52 mm after P side welding, and 0.86 mm after welding both sides.

3.2.4 In-plane deformation

Tables 3.2-2 and **3.2-3** summarize the measured in-plane deformation, which is defined as a change of dimension in the radial and circumference directions, respectively, due to the CP welding. Measurements after P side welding (the second column in Tables 3.2-2 and 3.2-3) seem to be excessive. The reason for this is not clear, but one possible explanation is error in the use of the micrometer which was developed especially for making these measurements. Therefore, a 3D measurement instrument used for measuring out-of-plane distortion, was used to measure in-plane deformation after welding the N side. Measured changes of the dimensions are sufficiently small after N side welding, as can be seen in Tables 3.2-2 and 3.2-3. And the ones at the center, WC1, WC2 and WC3, were found to be quite small. This is because the shrinkage of the RP mock-up, especially in the circumferential direction, is sufficiently small. Accordingly, it is also expected that any changes in the dimensions at the center also would be sufficiently small after P side welding. To correct the data after P side welding, it is assumed that the change of dimensions after P side welding would be zero at the center of the RP mock-up. Thus, the measured results are adjusted by subtracting the measured changes of dimensions at the center from the measured data, as may be seen in the third column in Tables 3.2-2 and 3.2-3. Note that the temperature at the time of measurement was 15 - 17 °C.

After P side welding, the width of the P plane shrank by 0.88 mm and that of the N side widened by 0.78mm in the radial direction, as measured at points WP2, WC2 and WN2. After N side welding, the width of the N plane shrank by 0.63 mm, and that of the P plane widened by 0.13 mm in the radial direction. The difference in these measurements is probably due to changes in the stiffness of the RP mock-up before and after P side welding. Deformation in the radial direction after CP welding is estimated to be between -1.2 and 0.3 mm.

After P side welding, the width of the P plane shrank by 0.27 mm, and that of the N plane widened by 0.39 mm in the circumferential direction, as measured at points LP2, LC2 and LN2. After N side welding, the width of the N plane shrank by 0.22 mm, and that of the P plane widened by 0.10 mm in the circumferential direction. The deformation in the circumferential direction after CP welding is estimated to be between -0.2 and 0.2 mm.

Deformation in the circumferential direction is much smaller than in the radial direction. This result indicates that the major in-plane deformation is shrinkage in width and bending of the RP mock-up.

Table 3.2-1 Summary of out-of-plane deformation

Measurement	Restraint	Measured plane	Maximum out-of-plane torsion [mm]
After P side welding	Fixed	P side	1.19
After P side welding	Released	P side	1.52
After N side welding	Fixed	N side	0.71
After N side welding	Released	N side	0.79
After N side welding	Released	P side	0.86

Table 3.2-2 Deformation in the radial direction

Measured point	After P side welding [mm]	After P side welding (adjusted) [mm]	After N side welding [mm]	After welding on both sides [mm]
WP1(P side)	1.62	-1.40	0.16	-1.24
WC1(Center)	3.02	0.00	-0.05	-0.05
WN1(N side)	3.69	0.67	-0.67	0.00
WP2(P side)	2.28	-0.88	0.13	-0.75
WC2(Center)	3.16	0.00	-0.02	-0.02
WN2(N side)	3.94	0.78	-0.63	0.15
WP3(P side)	2.62	-0.41	0.14	-0.27
WC3(Center)	3.03	0.00	-0.06	-0.06
WN3(N side)	3.71	0.68	-0.42	0.26

Table 3.2-3 Deformation in the circumferential direction

Measured point	After P side welding [mm]	After P side welding (adjusted) [mm]	After N side welding [mm]	After welding on both sides [mm]
LP1(P side)	2.71	-0.16	0.05	-0.11
LC1(Center)	2.87	0.00	-0.06	-0.06
LN1(N side)	3.15	0.28	-0.13	0.15
LP2(P side)	-1.16	-0.27	0.10	-0.17
LC2(Center)	-0.89	0.00	-0.02	-0.02
LN2(N side)	-0.50	0.39	-0.22	0.17
LP3(P side)	-3.21	-0.03	0.09	0.06
LC3(Center)	-3.18	0.00	0.00	0.00
LN3(N side)	-2.85	0.33	-0.24	0.09

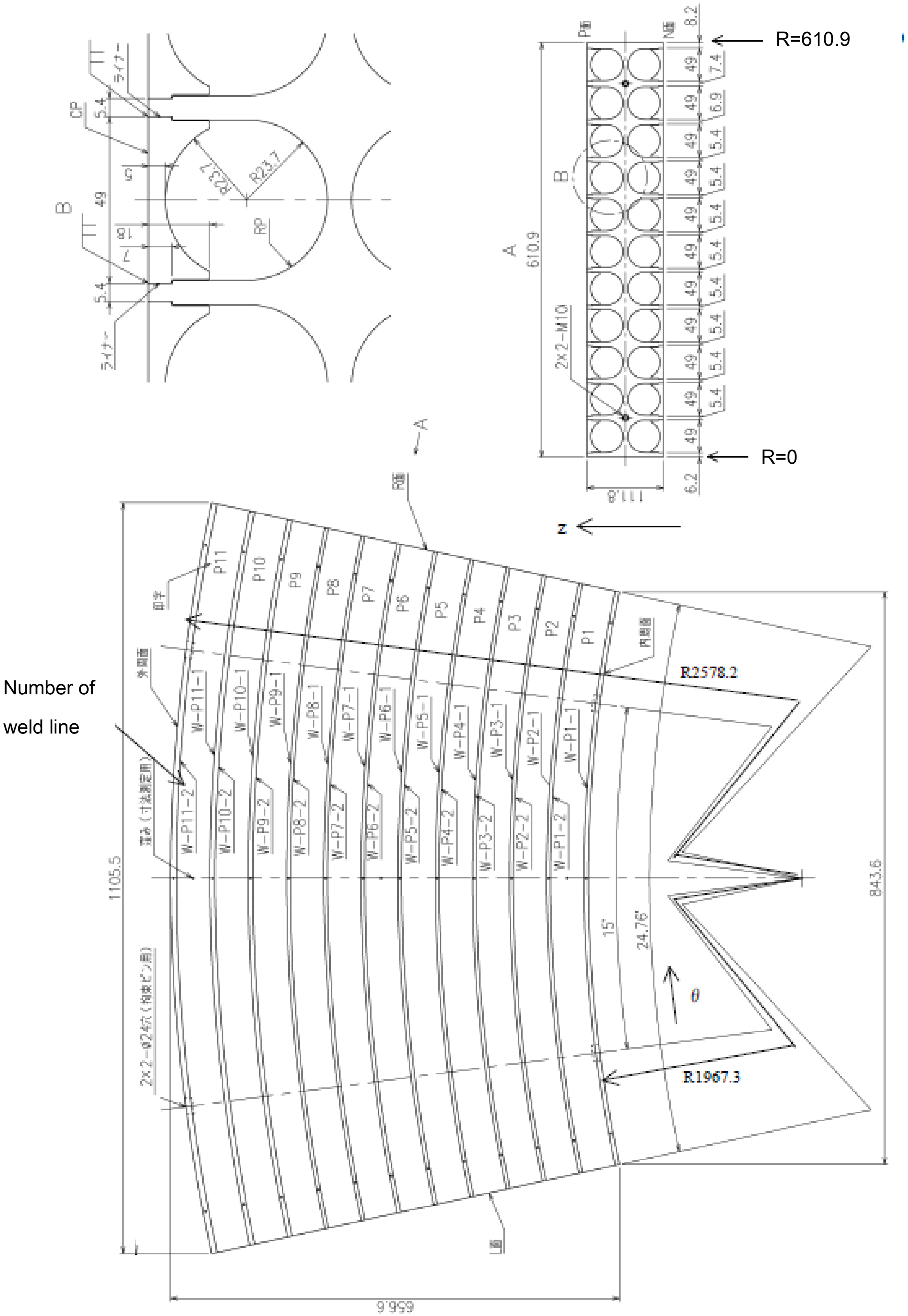

Fig.3.1-1 Dimensions of the RP mock-up

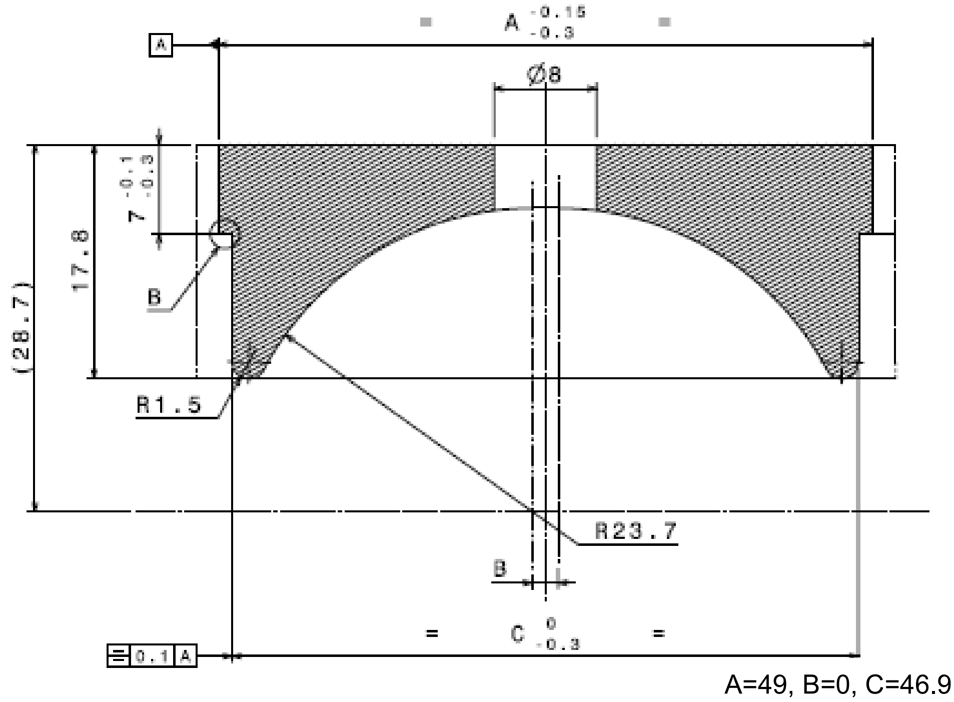

Fig.3.1-2 Dimensions of the CP

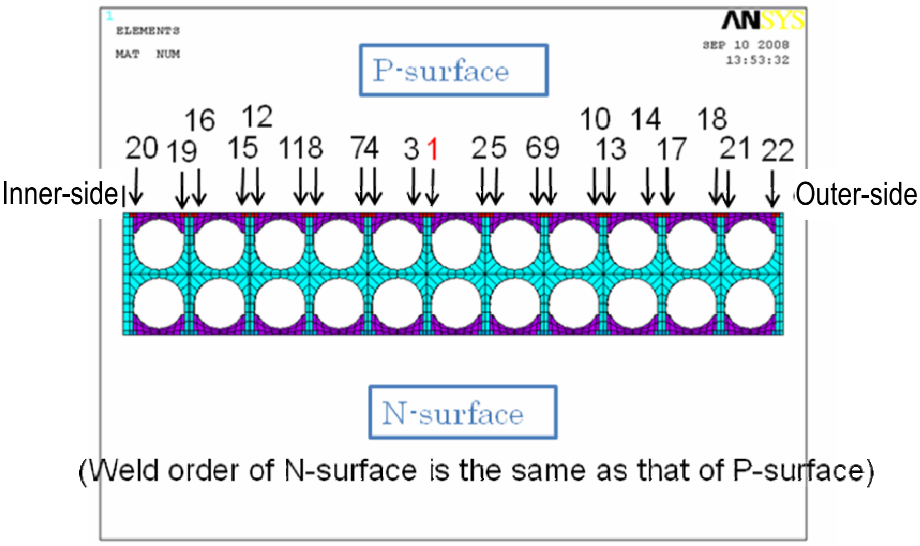

Fig.3.1-3 Welding sequence of the CP

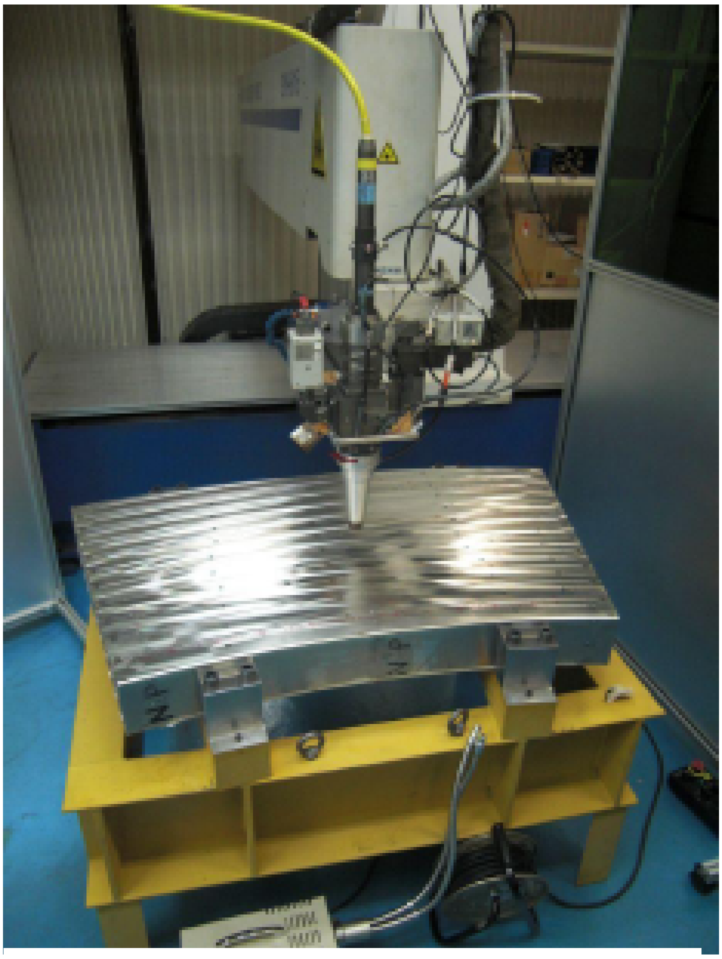

Fig.3.1-4 Laser welding machine

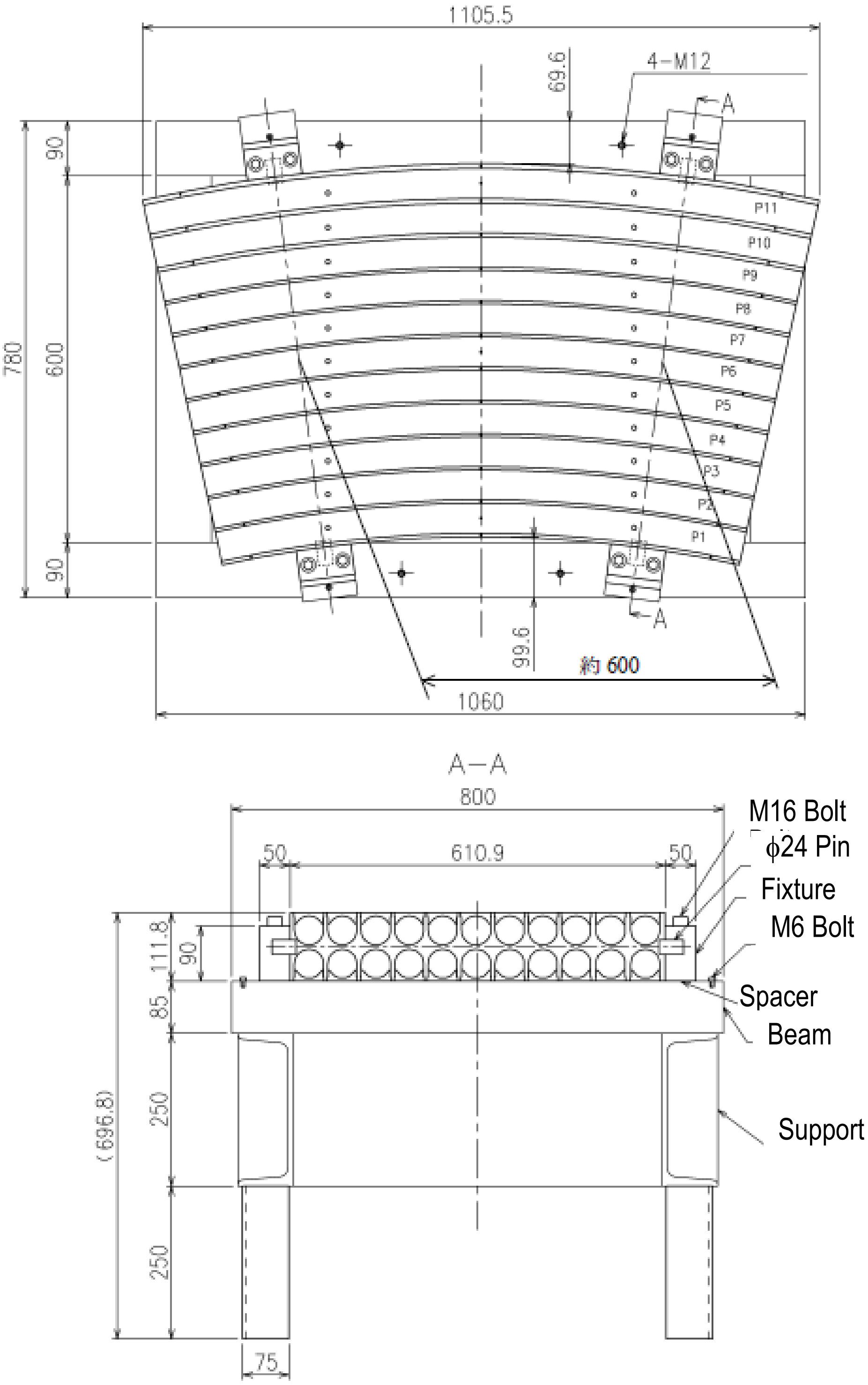

Fig.3.1-5 Restraint of the RP mock-up

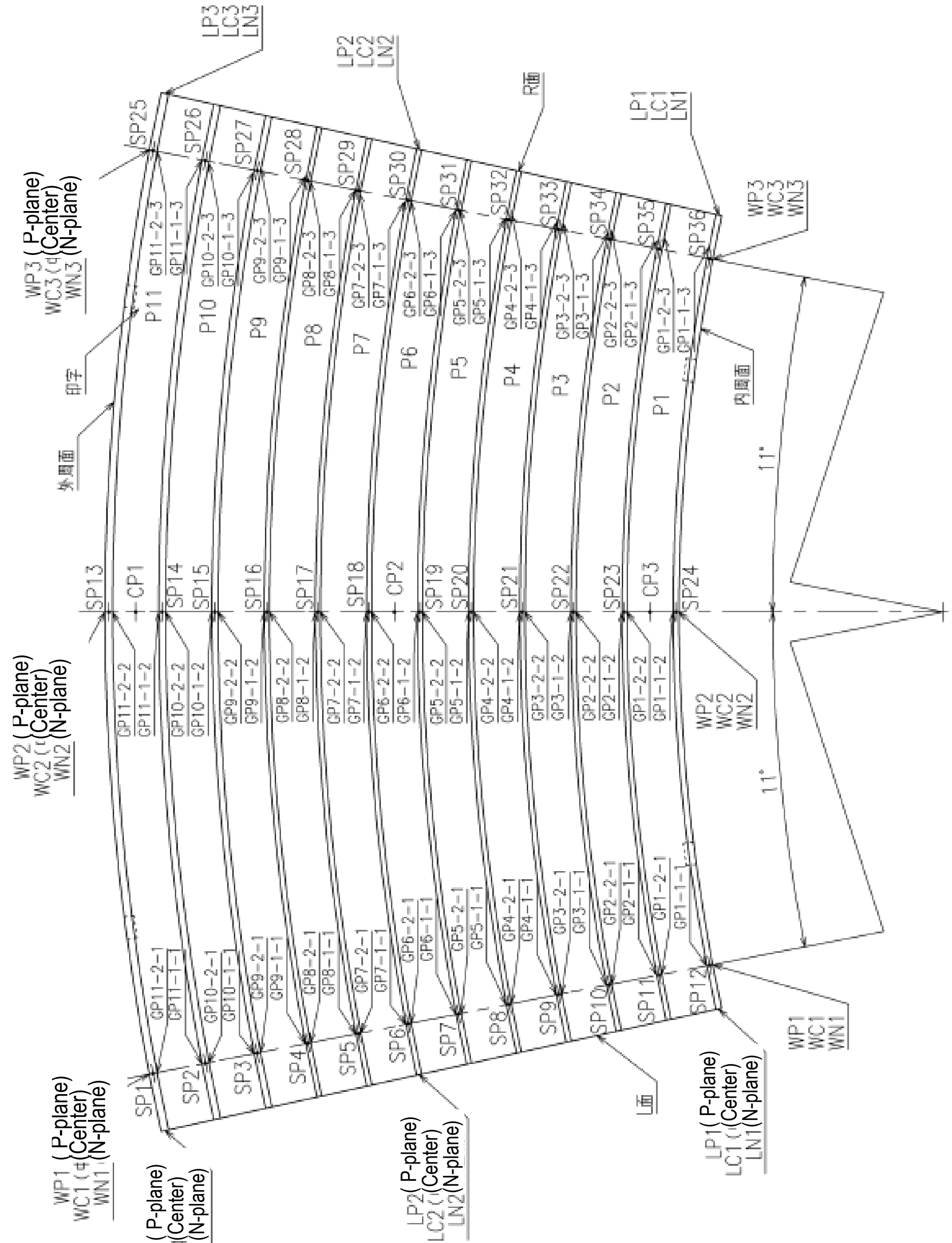

Fig.3.1-6 Points where deformations are measured

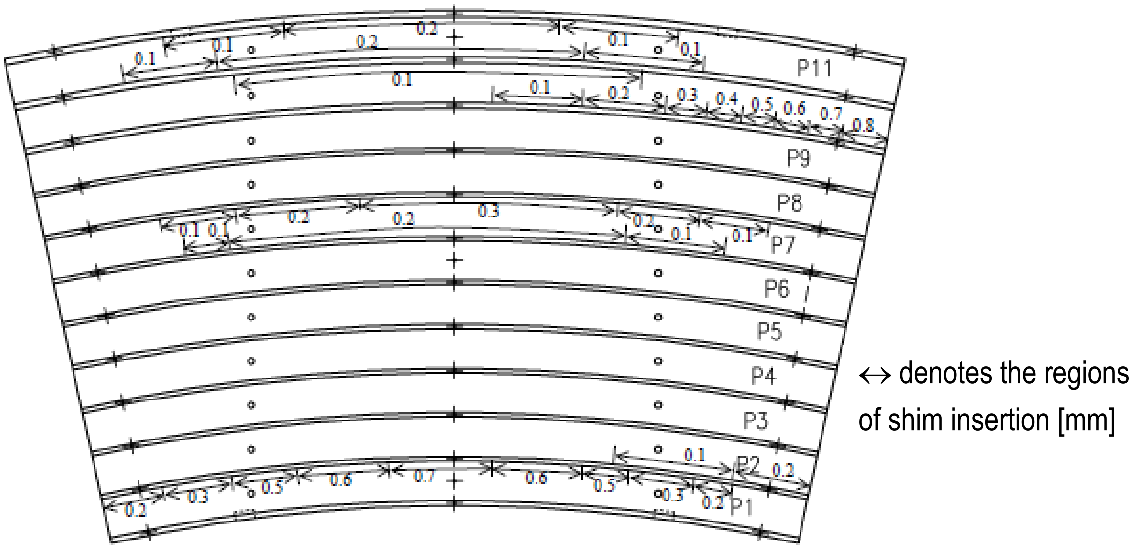

(a) P side

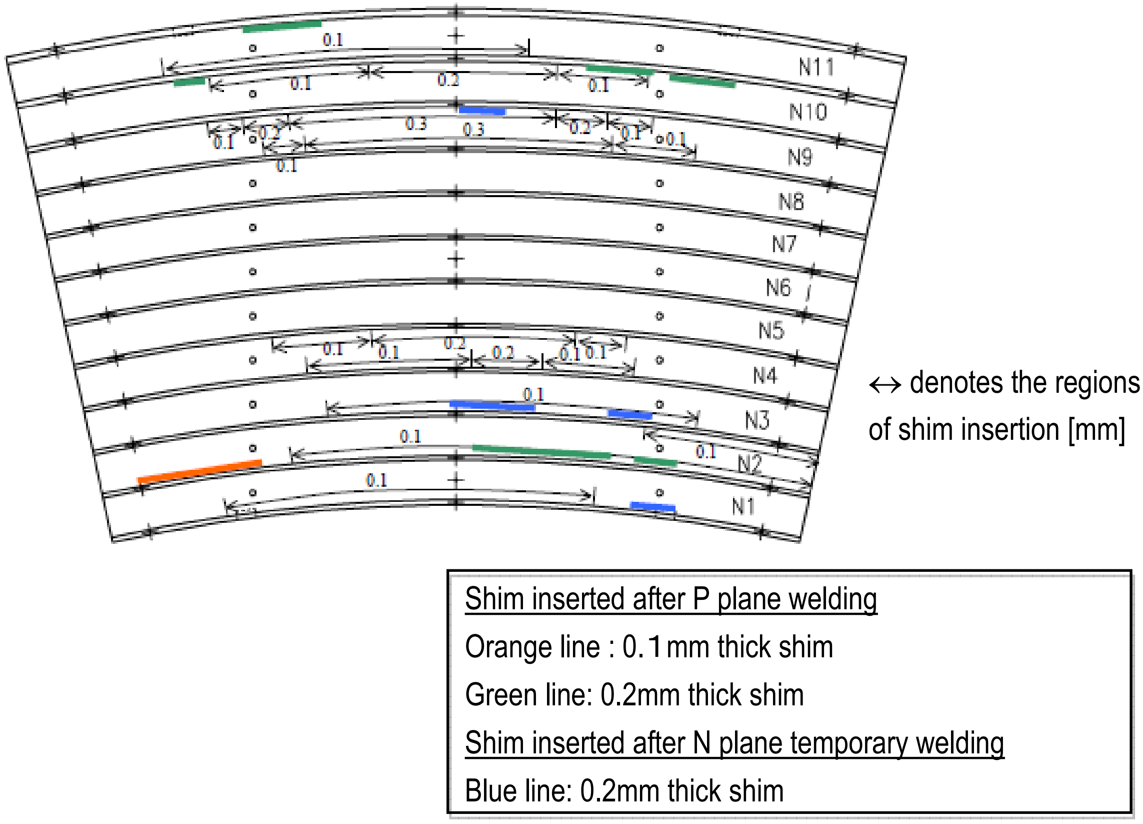

(b) N side

Fig.3.2-1 Locations where shims are inserted

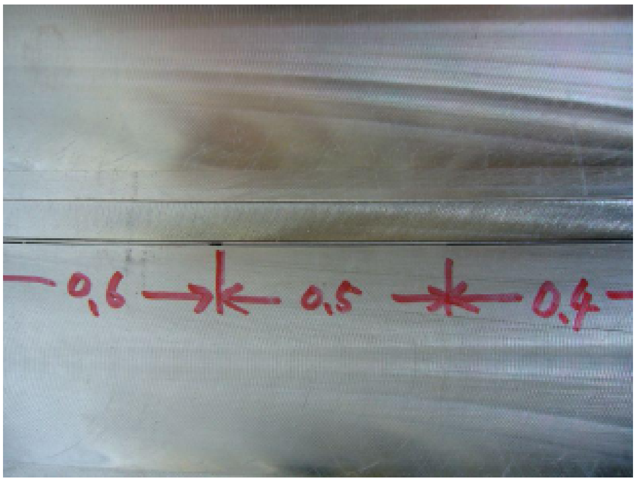

Fig.3.2-2 Inserted shims at P10-1 in Fig.7

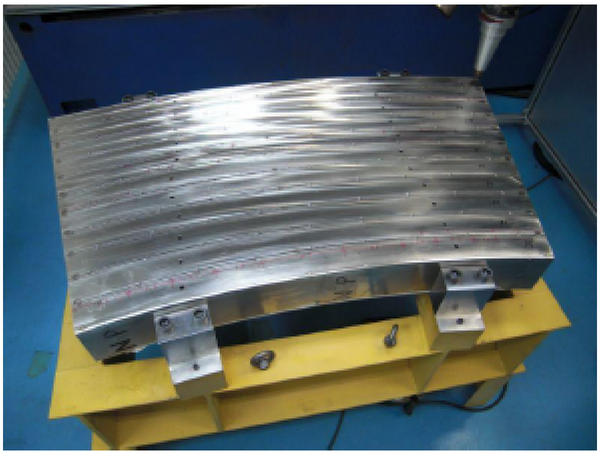

Fig.3.2-3 RP mock-up after laser tack-welding

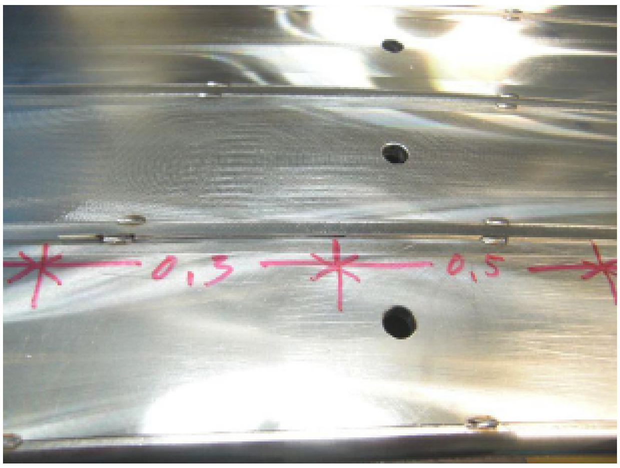

Fig.3.2-4 Laser tack-welding

Fig.3.2-5 Laser welding

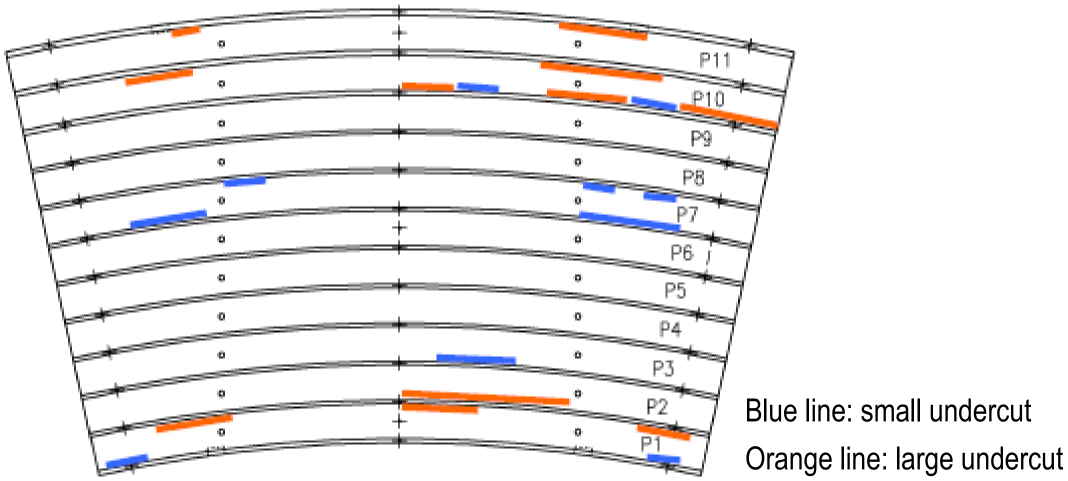

Fig.3.2-6 Record of undercutting of the welding bead after P side welding

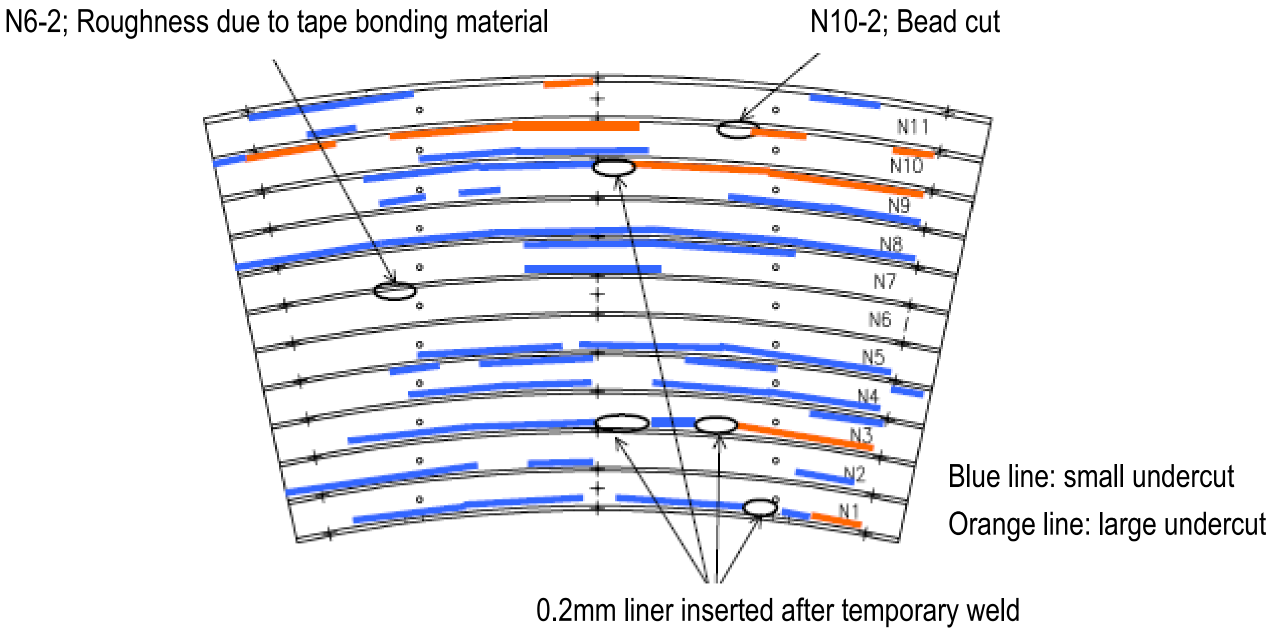

Fig.3.2-7 Record of undercutting of the welding bead after N side welding

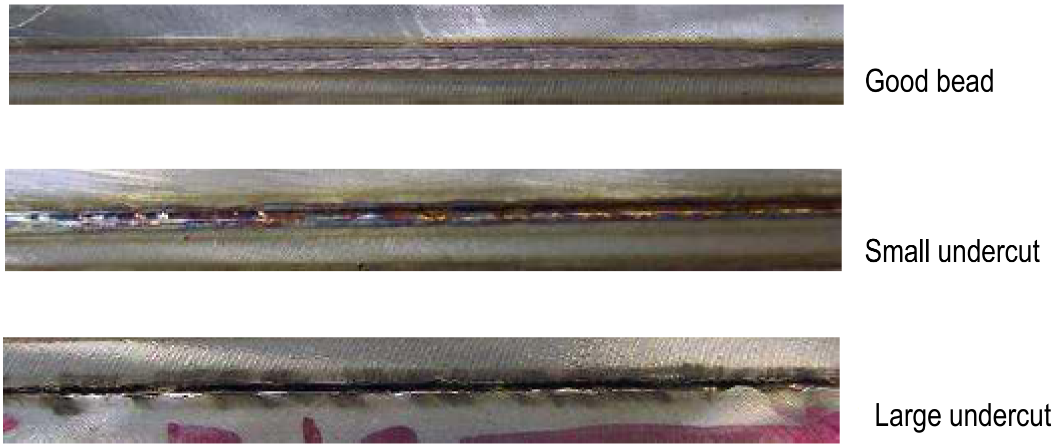

Fig.3.2-8 Comparison of welding beads

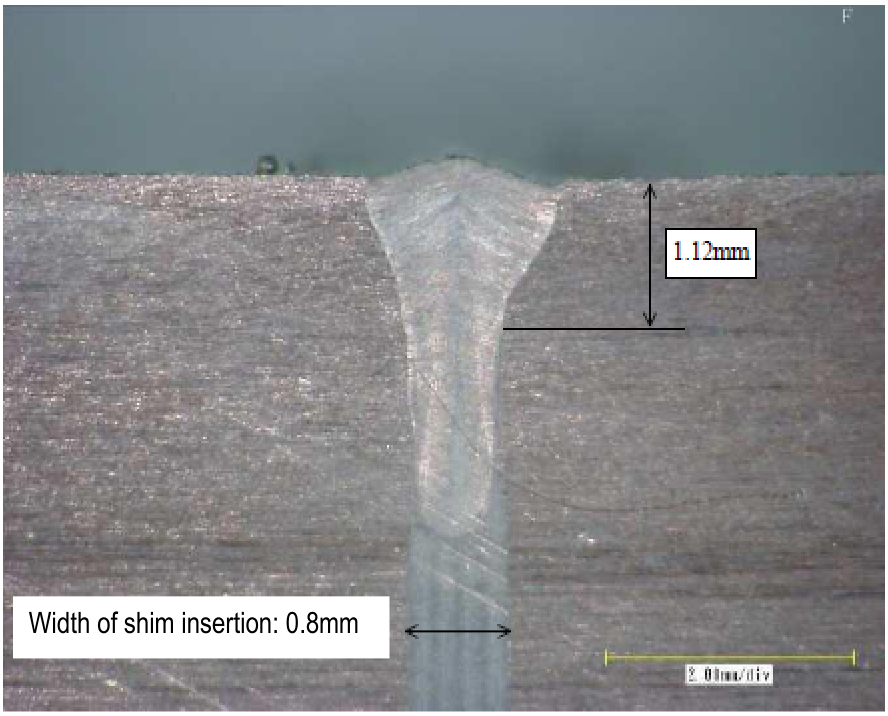

Fig.3.2-9 Cross section of a laser weld sample with 4 shims, each with a thickness of 0.2 mm

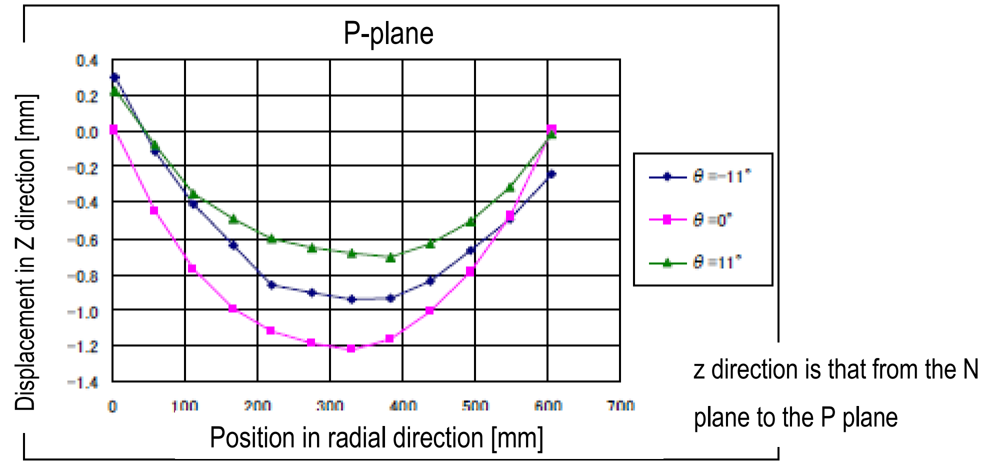

Fig.3.2-10 Out-of-plane deformation of the P plane without constraints after P side welding (difference in measurement before and after welding)

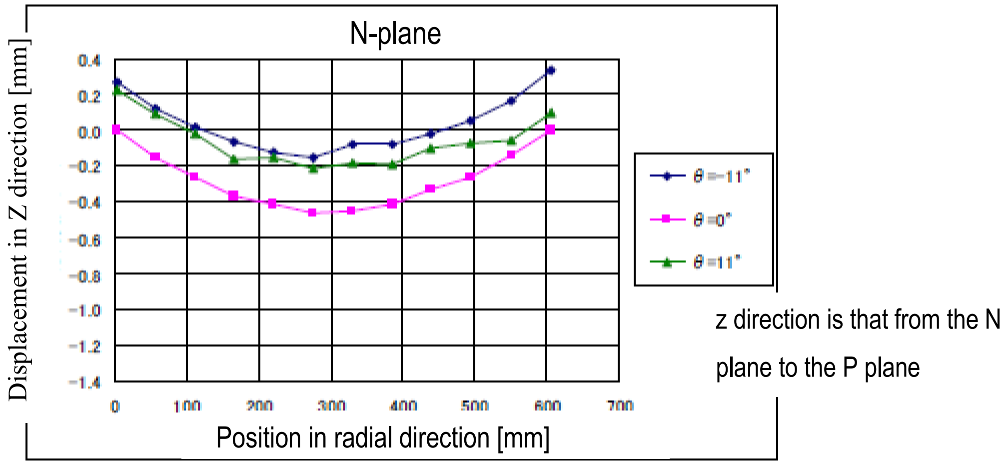

Fig.3.2-11 Out-of-plane deformation of the N plane without constraint after N side welding (difference in measurement before and after welding)

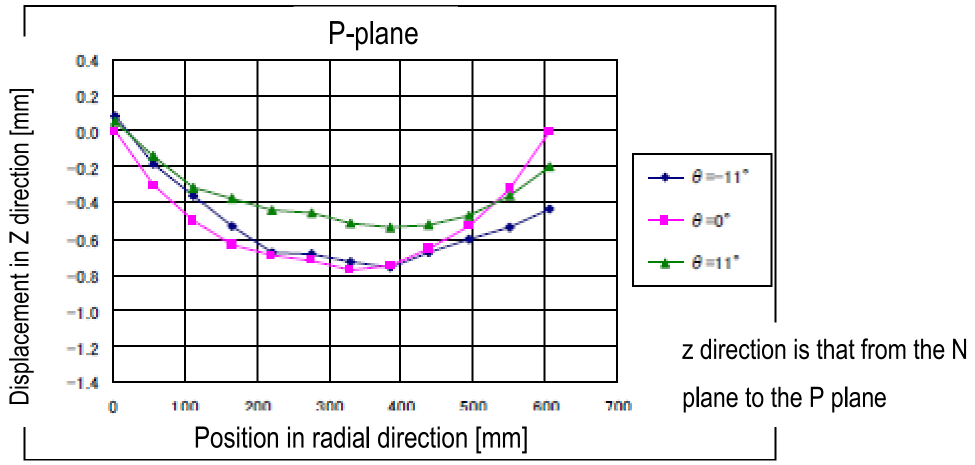

Fig.3.2-12 Out-of-plane deformation of the P plane without constraints after N side welding (difference in measurement before and after welding)

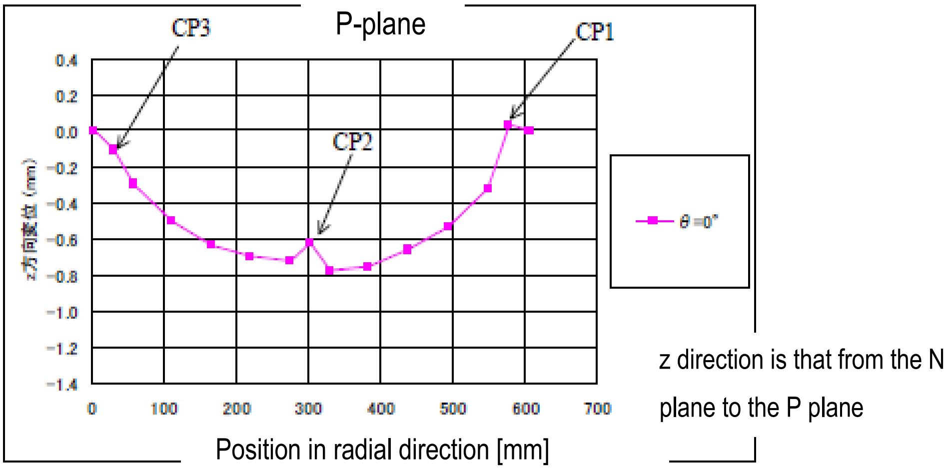

Fig. 3.2-13 Out-of-plane deformation of the P plane, including CP1 - CP3 on CP without constraint after P plane welding (difference in measurement before and after welding)

4. Analysis of the CP welding test of the RP mock-up

4.1 Method of analysis

4.1.1 Analytical model

Figure 4.1-1 shows an analytical model for the RP mock-up used in the CP welding test, described in the previous section. The welded regions of the model are simulated by rectangular elements measuring 7 mm wide and 3.5 mm thick, as shown in **Fig.4.1-2**. Note that the thickness of these elements was chosen to be 1 mm thicker than the welding thickness since the heat affected region is supposed to be 1 mm in our analysis. The welding sequence is the same as that in the test, which is shown in Fig.3.1-3. Material properties of the RP are 193GPa for Young's modulus and 0.3 for the Poisson ratio.

4.1.2 Boundary conditions

Boundary conditions are those shown in **Fig.4.1-3**. At the P side welding, the RP is affixed to the beams (Uz=0) by pins at the inner and outer sides, as may be seen in Fig. 3.1-5. The positions of the beams and pins are also shown in Fig. 3.1-5. During N side welding, the RP is assumed to be fixed by only pins along the inner and outer sides as a result of the distortion of the RP mock-up as is described in 3.1.3.

4.1.3 Analytical sequence

The analytical sequence is as follows:

(1) Welding on the P side,
(2) Releasing the restraint,
(3) Welding on the N side, and
(4) Releasing the restraint.

Inherent strains are applied on a single welding line simultaneously. The nodes of the welding line are connected between the CP and the RP teeth by constraint equations. The length of tack-laser welding is 100 mm, and no welding deformation is assumed for tack-laser welding.

4.1.4 Determination of inherent strain

Since the gaps between the CP and RP teeth have relatively large variation along each welding line, as mentioned previously, inherent strain changes accordingly. Therefore, welding deformation exhibits some variation compared to the deformation that occurs when inherent strains are constant. However, it is quite difficult to take the variation of inherent strain into account. Consequently, constant inherent strain is assumed in our analysis, for the sake of simplicity. This assumption makes it almost impossible to obtain a complete fit between calculated welding deformation and measured results. Thus, the inherent strains are determined by fitting the welding deformation calculated at certain representative points to measured values. The distortions and displacement at the center of the RP mock-up in the circumferential direction (measurement points: LP2 and LN2) are selected as the data to be fitted. Note that displacement in the radial direction is not selected as a fitting parameter. The estimated inherent strains are listed in **Table 4.1-1**.

The estimated inherent strains are smaller on the N side than on the P side. One possible explanation for this is a widening of the gap between the CP and the RP teeth as a result of P side welding. This gap may reduce welding thickness, as may be seen in Fig.3.2-9, resulting in smaller heat input into the base material. Another possible explanation for the gap is insertion of shims after P side welding. From these results, it may be concluded that the inherent strain listed in Table 4.1-1 gives the worst case for out-of-plane distortion.

4.2 Calculation results

The calculation results show that the CP is distorted by 1 mm, although the measured distortion of the CP is only 0.1 mm. This large distortion is probably attributable to the relatively large element on which inherent strain is applied when compared to the size of the CP. Consequently, the distortion of the CP in the calculation is ignored in the following procedures in the attempt to estimate welding deformation .

Comparisons of out-of-plane distortion of the test and calculation results are listed in **Figs. 4.2-1** and **4.2-2**. The calculated and measured maximum distortions are shown in **Table 4.2-1**. Since the distortion of the RP mock-up is complicated as a result of non-uniform welding conditions, and the plane of reference against which to measure distortions is not clear after the release of the restraints, the out-of-plain displacement of the tested RP mock-up is defined as the distance from the base plane comprised of three points chosen from four corners of the RP mock-up.

Calculated distortions show good agreement with those of the test results, yielding an accuracy of ±0.01mm at points LP2 and LN2 in Fig.3.1-6. Since these values are the fitted parameters, this agreement seems natural. However, the tendencies of the calculated out-of-plane displacement are in relatively good agreement with those of the test results, as can be seen in Figs. 4.2-1 and 4.2-2.

Displacements in the circumferential direction of measured and calculated values are shown in **Fig. 4.2-3** and **Table 4.2-2**. Bold numbers in Table 4.2-2 are used to determine the inherent strains. **Figure 4.2-4** and **Table 4.2-3** show displacement in the radial direction. Both calculated circumferential and radial displacements show relatively good agreement at all points, although the displacement only in the center of the radial plate in the circumferential direction and the distortion are fitted.

Table 4.1-1 Thermal expansion coefficients and inherent strain

	Thermal expansion coefficient [$\times 10^{-6}$ 1/K]			Inherent strain (dT=-1500°C)		
	αx width direction	αx θ direction	αx thickness direction	αx·dT	αx·dT	αx·dT
P side weld	82	7	-50	-0.123	-0.011	0.075
N side weld	63	6	-50	-0.095	-0.009	0.075

Table 4.2-1 Comparison of out-of-plane distortion between test and calculation results (measured plane: P side) [mm]

	Test results	Calculation results
After P side weld and constraint released	1.52	1.53
After P side weld and constraint released	0.86	0.85

Table 4.2-2 Comparisons of circumferential displacement between the test and calculation results (measured plane: P side) [mm]

	Test results		Calculation results	
Measurement point	Dimension change after P side weld	Dimension change after N side weld	Dimension change after P side weld	Dimension change after N side weld
LP1(P side)	-0.16	0.05	-0.01	0.04
LC1(Center)	0.00	-0.06	-0.09	-0.08
LN1(N side)	0.28	-0.13	0.08	0.00
LP2(P side)	**-0.27**	0.10	**-0.27**	0.04
LC2(Center)	0.00	-0.02	-0.04	-0.04
LN2(N side)	0.39	**-0.22**	0.07	**-0.21**
LP3(P side)	-0.03	0.09	-0.30	0.05
LC3(Center)	0.00	0.00	0.01	0.00
LN3(N side)	0.33	-0.24	0.05	-0.24

Bold numbers are used for determining the inherent strains.

Table 4.2-3 Comparison of radial displacement between the test and calculation results (measured plane: P side) [mm]

Measurement Point	Test results		Calculation results	
	Dimension change after P side weld	Dimension change after N side weld	Dimension change after P side weld	Dimension change after N side weld
WP1(P side)	-1.40	0.16	-1.57	0.09
WC1(Center)	0.00	-0.05	0.04	-0.03
WN1(N side)	0.67	-0.67	0.67	-1.10
WP2(P side)	-0.88	0.13	-1.92	0.10
WC2(Center)	0.00	-0.02	0.04	-0.05
WN2(N side)	0.78	-0.63	0.69	-1.62
WP3(P side)	-0.41	0.14	-1.98	0.10
WC3(Center)	0.00	-0.06	0.03	-0.04
WN3(N side)	0.68	-0.42	0.74	-1.40

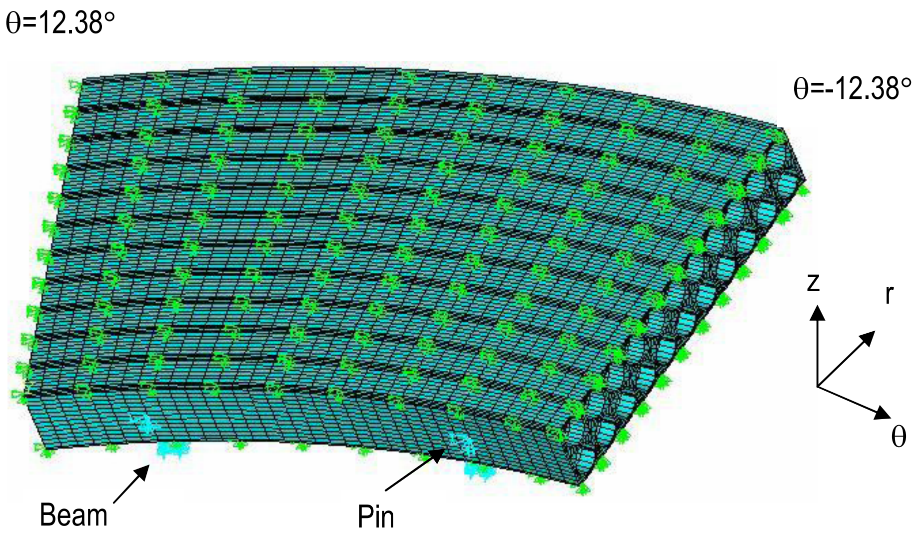

Fig.4.1-1 Analytical model of the weld test

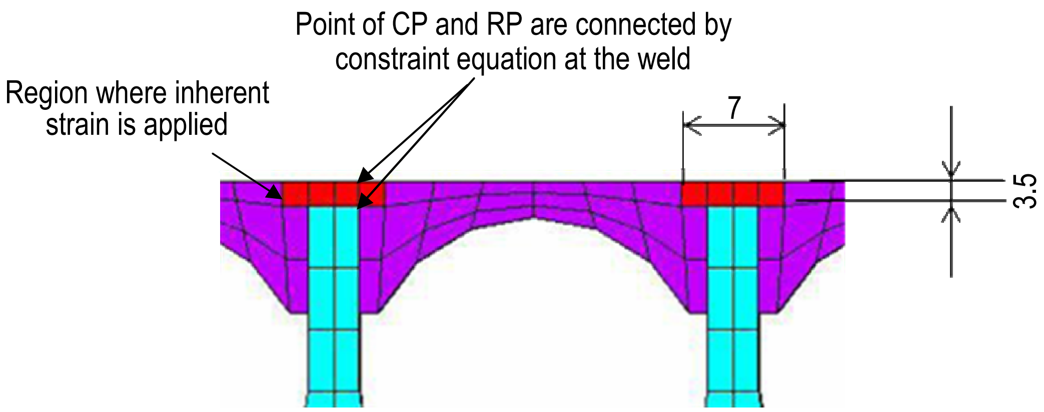

Fig.4.1-2 Analytical model of the weld region

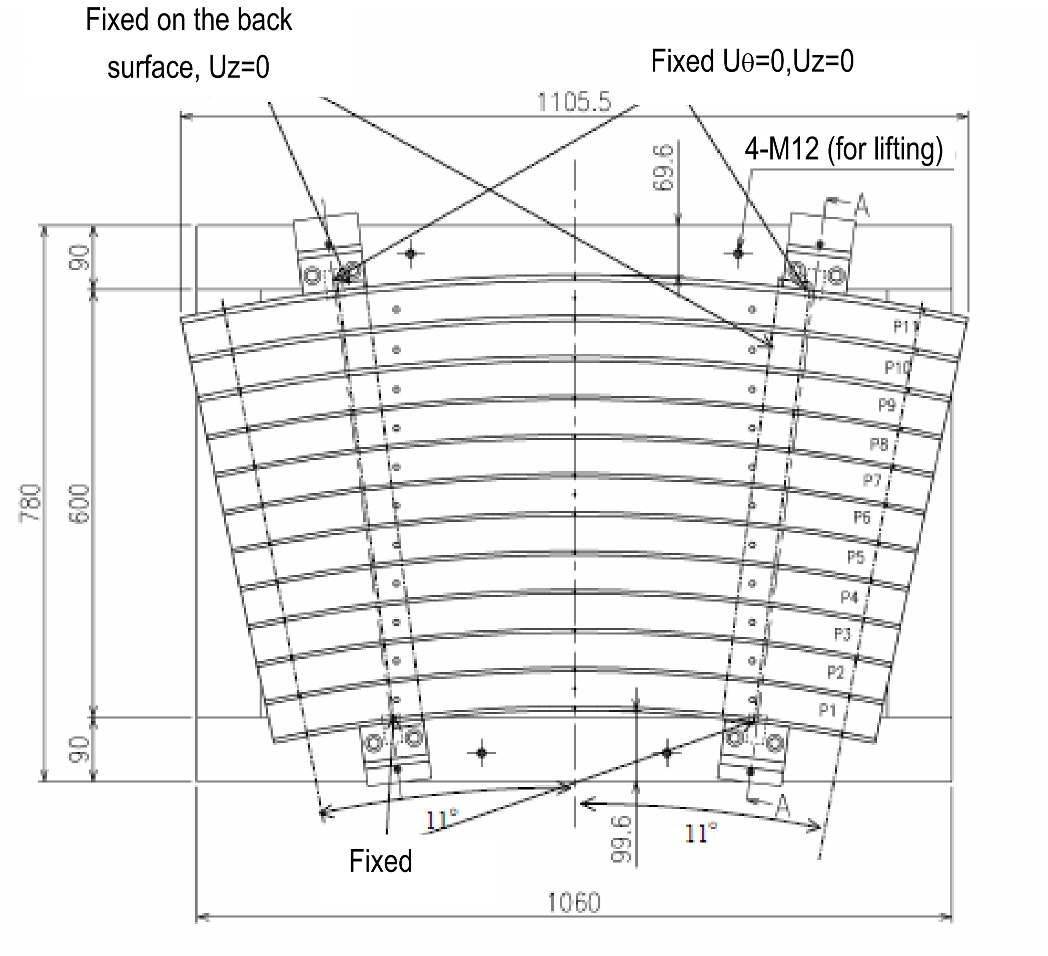

Fig.4.1-3 Boundary condition

Out-of-plane deformation of P side after P side welding

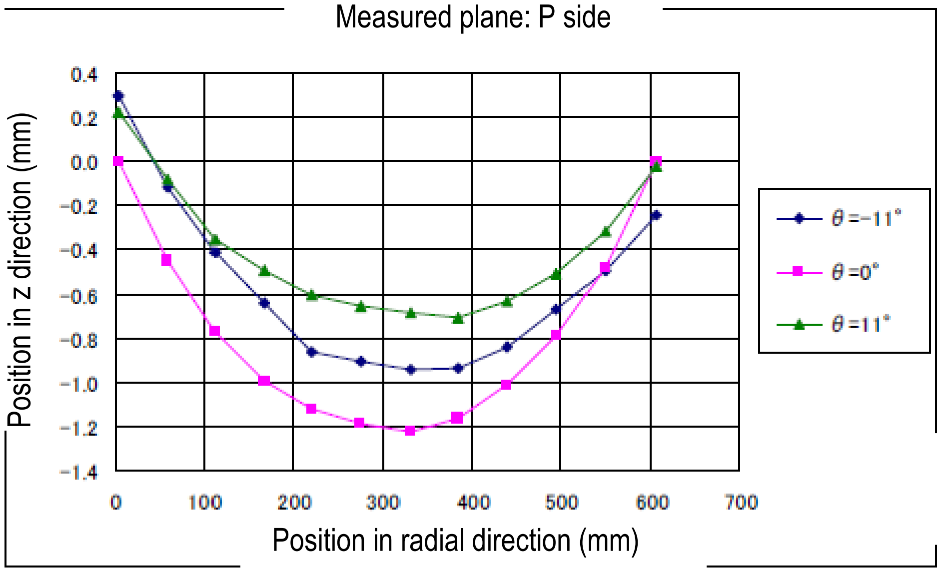

(a) Test results

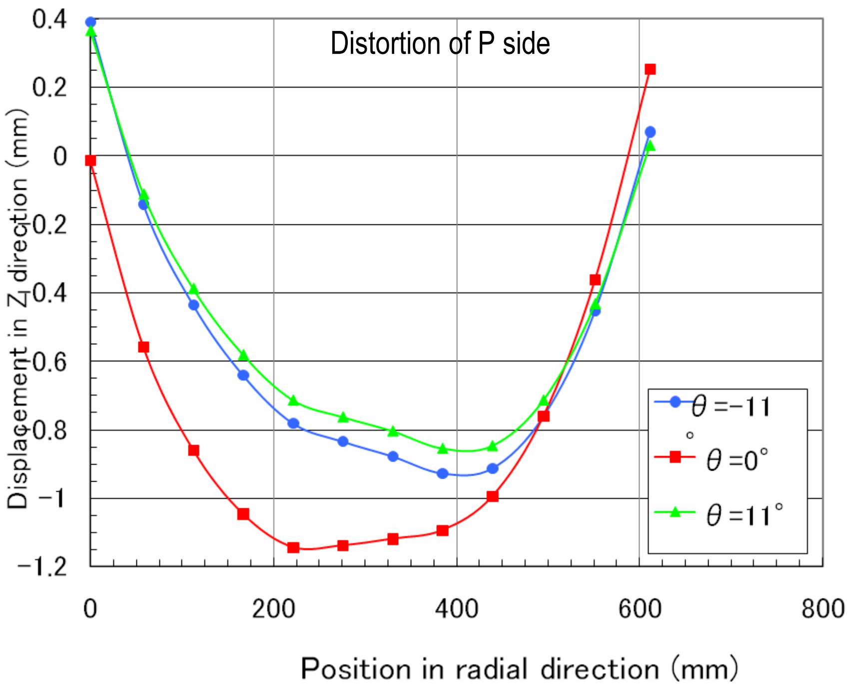

(b) Analytical results

Fig.4.2-1 Comparison of out-of-plane distortion after P side welding and release of the restraints of the RP mock-up (Deformation of the P side in the out-of-plane direction)

Out-of-plane deformation of the P side after N side welding

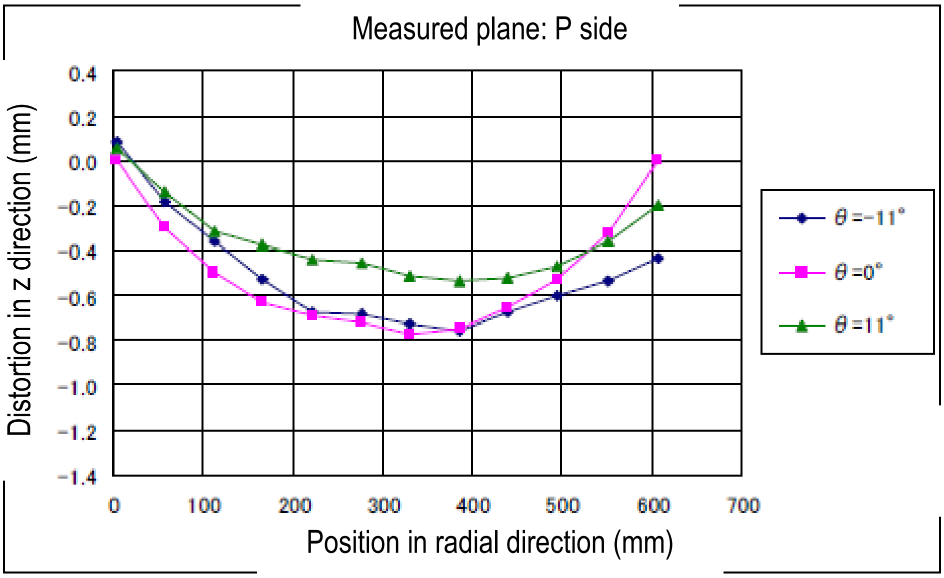

(a) Test results

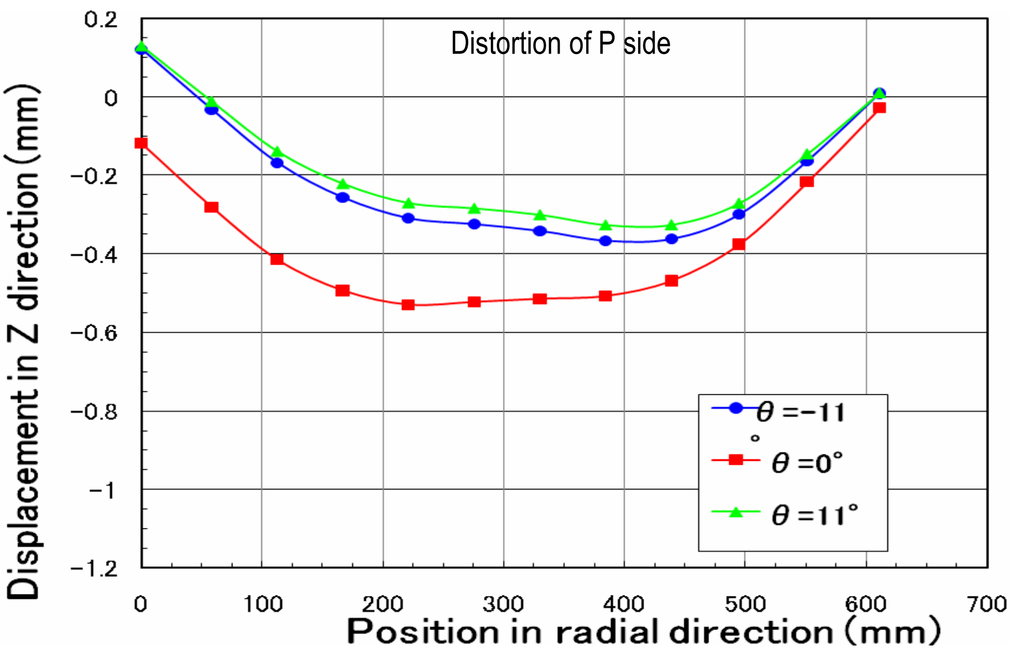

(b) Analytical results

Fig.4.2-2 Comparison of out-of-plane distortion after N side welding and release of the restraints of the RP mock-up (Displacement in the out-of-plane direction)

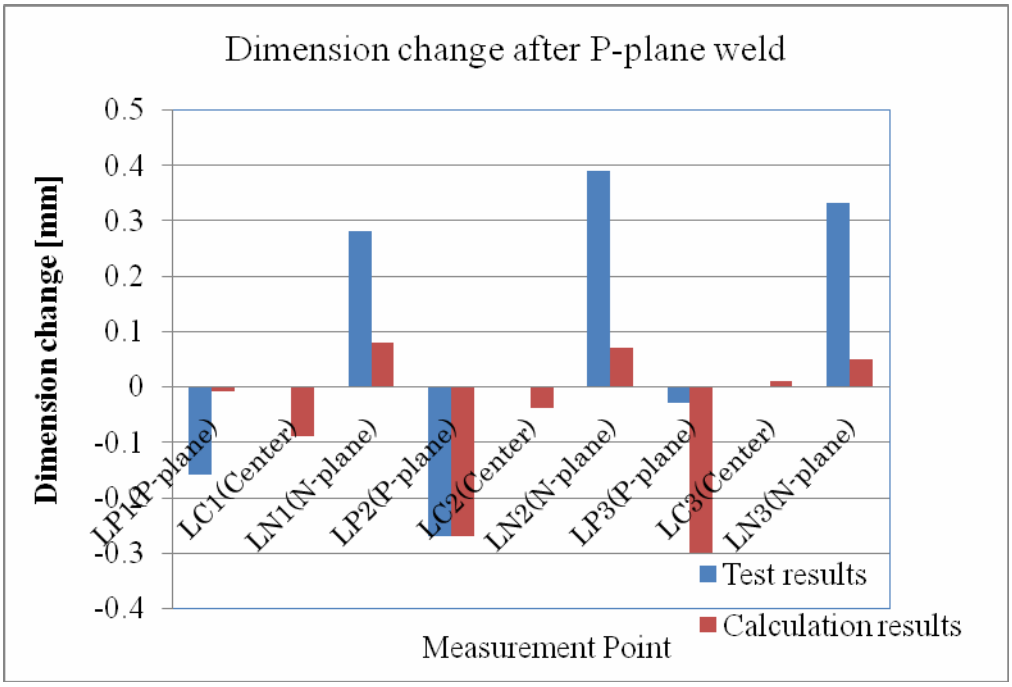

(a) Circumferential dimension change after P side welding

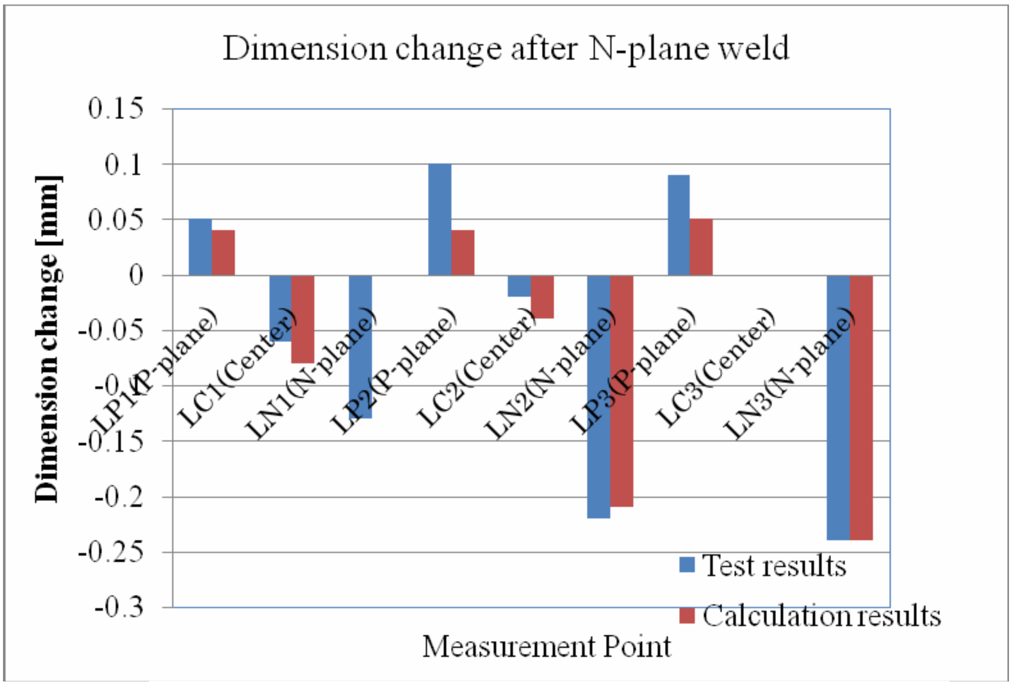

(b) Circumferential dimension change after N side welding

Fig.4.2-3 Comparison of circumferential displacement after P side and N side welding and release of the restraints of the RP mock-up (Measurement on the P side)

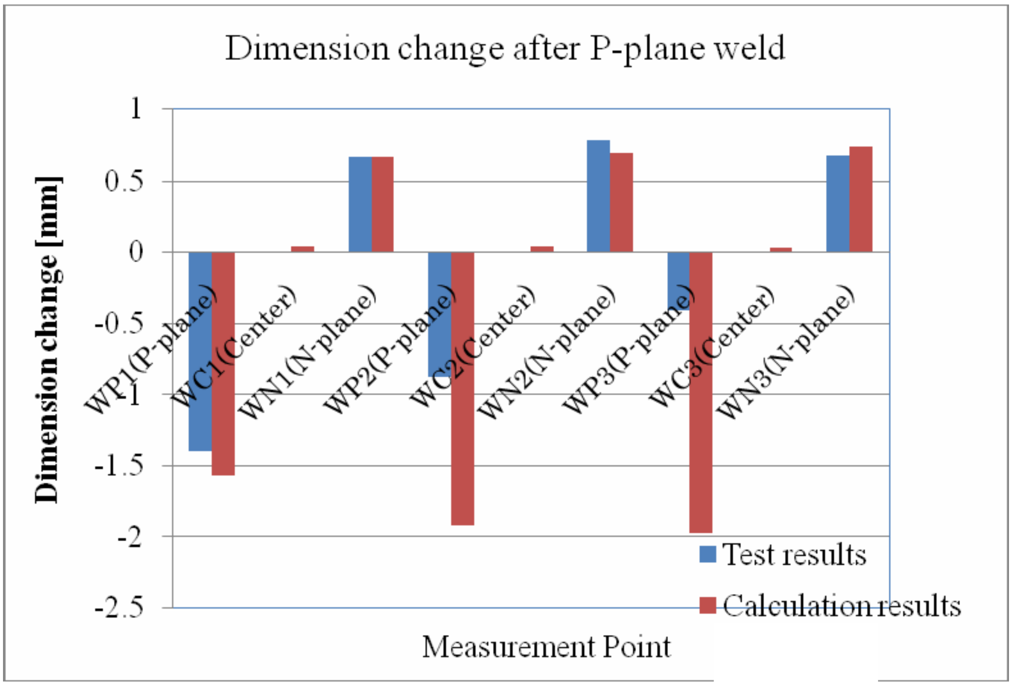

(a) Radial displacement after P side welding

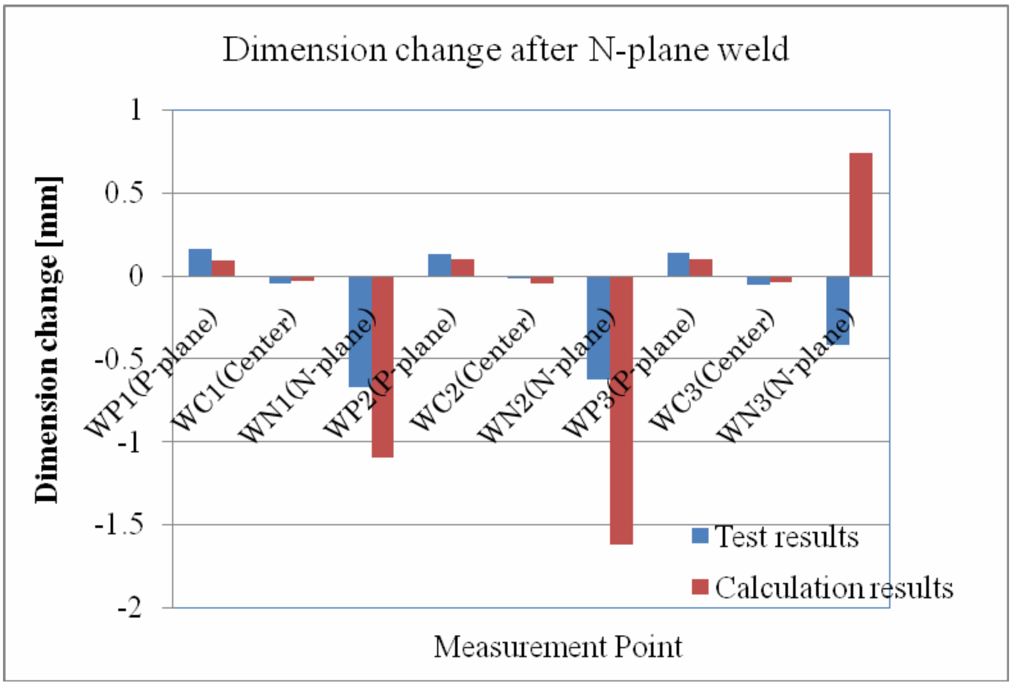

(b) Radial displacement after N side welding

Fig.4.2-4 Comparison of radial displacement after P side and N side welding and release of the RP mock-up (measurement on the P side)

5. Analysis of CP welding deformation of a full scale RP
5.1 Method of analysis
5.1.1 Analytical model

A half-scale RP, shown in **Fig.5.1-1**, is assumed as a model to estimate deformation of the RP, for the sake of simplicity, because the RP is almost symmetrical on the equatorial plane. Material properties of the RP are 193 GPa for Young's modulus and 0.3 for the Poisson ratio. Analysis was performed for the following two cases:

1) Welding between CPs and the RP teeth. In addition, the effect of various parameters is studied in this case.
2) Welding between adjacent CPs.

Details about these models are written in below.

(1) Welding between CPs and RP teeth

The mesh shown in **Fig.5.1-2** is used in this calculation. Welded regions are modeled by rectangular elements, 7 mm wide and 3.5 mm thick, for cases in which the welding thickness is 2.5 mm, as well as for the RP mock-up.

The welding sequence is the same as that of the welding test, which is shown in Fig.3.1-3. No welding between CPs is included in this model.

The cross sections of the RP are slightly different between inboard and outboard regions. In order to study the effect of the different cross sections, analyses are performed for both cross sections.

In addition, preliminary analyses indicate that when an in-plane deformation is attributed to bending, a reduction in welding thickness at the curved region also is affected. Therefore, the effect of the welding thickness at the curved region is also studied.

(2) Welding between CPs

The analytical model shown in **Fig.5.1-3** is used to estimate the deformation due to welding between CPs. The welding sequence is also shown in **Fig.5.1-3**. No welding between CPs and RP teeth are included in this model. The inherent strains used in these analyses are assessed when the P side is welded, as shown in **Table 5.1-1**,.

5.1.2 Boundary conditions

As shown in **Fig.5.1-4**, the boundary conditions are as follows:

For P side welding:

1) Upoloidal=0 and Ur=0 at the inner edge where the RP is restrained
2) Upoloidal =0 at the outer edge where the RP is restrained
3) Uy=0 at the bottom of the RP

The restraint interval is 600 mm.

For N side welding, the boundary conditions are the same as those for the P side welding except for condition 3).

5.1.3 Inherent strain

The inherent strains used in this analysis are listed in **Table 5.1-1**. Two cases of inherent strain are assumed. The first assumption is that the inherent strains are identical for both the P and N sides. This assumption is fulfilled when identical welding conditions are maintained on both sides. As such, the assumption may be optimistic. The welding sequence should be determined so as to achieve this target. The other assumption is that some inherent strains differ between the P and N sides. Inherent strains are estimated from the results of the welding test in which some spacers were inserted into gaps greater than 0.2mm between the CP and RP teeth prior to N side welding. These gaps were produced by insufficient restraint during the N side welding. Such asymmetrical procedures probably cause a large discrepancy in estimating the inherent strains between the N and P sides. Therefore, this case may be pessimistic.

Thus, analysis is done to study the following effects:

1) Effect of cross section: Model 1 (inboard cross section model) and Model 2 (outboard cross section model).
2) Effect of the same and different inherent strains on the P and N sides: Models 1 and 3 are for the inboard cross section, and Models 2 and 4 for the outboard cross section
3) Effect of a reduction in the welding thickness to 1 mm at the curved region: Model 5
4) Effect of welding between CPs : Model 6

The model number and the corresponding conditions of analysis are summarized in **Table 5.1-2**. The welding elements in FEM analysis are assumed to be 3.5mm and 2.0mm for weld depths of 2.5mm and 1.0mm, respectively, including a heat affected zone of 1.0mm, as mentioned previously.

5.2 Analytical results

5.2.1 Weld deformation of the reference design

The calculated welding deformations for Model 1 are shown in **Table 5.2-1**. After P side welding and removal of the restraints, the out-of-plane distortion is 35.3 mm. After N side welding and removal of the restraints, the distortion decreases to 2.4 mm, which is in the range of the tolerance level of 2 mm. The largest displacements in the radial and vertical directions are -8.0 mm and -3.6 mm, respectively. Distribution of displacement after N side welding and restraint release is shown in **Figs. 5.2-1** – **5.2-3**. **Fig 5.2-4** shows the calculated displacement of the contour in the middle of the height of the RP. This result confirms that in-plane deformation is mainly attributed to the bending of the RP. In fact, the shrinkage of the average length of the RP is estimated as only 0.01%, which corresponds to about 1 mm displacement in the horizontal direction, while the actual horizontal displacement is evaluated as being more than 6 mm.

Comparing the displacement of Model 1 with the inboard cross section to that of Model 2 with the outboard cross section, there is little difference in in-plane deformation. The out-of-plane distortion of Model 2 with the outboard cross section is two-thirds that of the inboard cross section.

5.2.2 Effect of the different inherent strains between the P and N sides

The best fitted inherent strains are different between the P and N sides, as mentioned previously. The welding conditions between the P and N sides should be the same to reduce distortion. However, welding conditions might be different for each side during the actual welding process. Therefore, analyses of the different inherent strains between the P and N sides have been performed to study this effect. Note that these analyses may represent a worst case scenario in terms of out-of-plane distortion.

Welding deformation for the different inherent strains is shown in **Table 5.2-2**. In-plane deformations for those inherent strains judged unique to each side are slightly smaller compared to the inherent strains judged to be the same for each side. This result may stem from the fact that the inherent strains on the N side are smaller.

In contrast, the out-of-plane deformation of the inherent strains unique to each side is larger than that for identical inherent strains. This is obviously because of the asymmetry of inherent strains. Out-of-plane distortions of all cases exceed the tolerances for flatness. It is therefore important to make the welding conditions of the P and N sides the same; namely, to restrain out-of-plane distortion sufficiently during P side welding and to suppress final out-of-plane deformation.

5.2.3 Effect of a reduction in welding thickness to 1mm at the curved region

Analytical results for the model (Model 5) in which the welding thickness is assumed to be 1mm at the curved region are listed in **Tables 5.2-3** and **5.2-4**. **Fig 5.2-5** shows the calculated displacement of the contour in the middle of the height of the RP. Displacement in all directions is reduced from those of the reference design. A reduction in weld thickness makes the in-plane welding deformation smaller. Reducing the welding thickness at the curved region therefore seems to be a promising solution that satisfies the required tolerances regarding in-plane deformation.

On the other hand, the reduction in out-of-plane distortion is minimal. This result may be due to shrinkage near the RP surface which affects the out-of-plane distortion due to bending.

5.2.4 Welding deformation by welding between CPs

The calculated deformation from welding between CPs is listed in **Table 5.2-5**. After N side welding and release of the restraints, the displacement due to welding between CPs is sufficiently small compared to the displacement due to welding between the CPs and the RP teeth. We therefore conclude that welding deformation between CPs has a minimal effect on the welding deformation of the RP.

Table 5.1-1 Thermal expansion coefficients and inherent strain

Case under Analysis		Thermal expansion coefficient [$\times 10^{-6}$ 1/K] (dT=-1500°C)			Inherent strain		
		αx width direction	αx θ direction	αx thickness direction	αx·dT	αy·dT	αz·dT
(1) Same strains for P and N sides	P and N sides	82	7	-50	-0.123	-0.011	0.075
(2) Different strains for P and N sides	P side	82	7	-50	-0.123	-0.011	0.075
	N side	63	6	-50	-0.095	-0.009	0.075

Table 5.1-2 Analytical models for the full scale RP

Model No.	Inherent strains for P and N sides	Cross section of FEM model	No. of weld lines on one side	Welding thickness	Depth of FEM weld elements
Model 1	Same strains	Inboard	Poloidal : 22	2.5mm	3.5mm
Model 2		Outboard	Poloidal : 22	2.5mm	3.5mm
Model 3	Different strains	Inboard	Poloidal : 22	2.5mm	3.5mm
Model 4		Outboard	Poloidal : 22	2.5mm	3.5mm
Model 5	Same/different strains	Inboard	Poloidal : 22	Straight 2.5mm Curved 1mm	Straight 3.5mm Curved 2mm
Model 6	Same strains	Inboard	Radial : 14	2.5mm	3.5mm

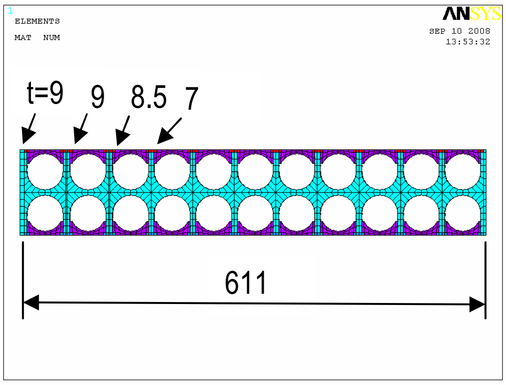

(a) Inboard cross section

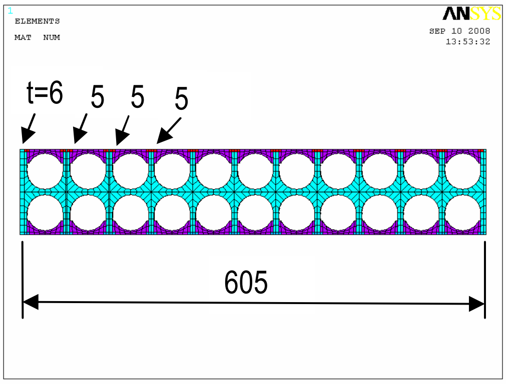

(b) Outboard cross section

Table 5.2-1 Deformation of a real RP assuming the same inherent strains for the P and N sides

Model No.	Condition	Ux (radial)	Uy (thickness)	Uz (vertical)
Model 1(Ref. inboard)	After P side welding and restraint removal	-2.06/0.01 /2.07	-0.36/34.87 /35.23	0/0.39 /0.39
Model 2(Ref. outboard.)		-2.29/-0.03 2.32	-0.26/19.00 /19.26	0/0.37 0.37
Model 1(Ref. inboard)	After N side welding and restraint removal	-4.71/0.05 /4.76	-0.51/0.27 /0.78	-0.11/0.67 /0.78
Model 2(Ref. outboard.)		-4.90/0.02 /4.92	-0.29/0.20 /0.49	-0.08/0.72 /0.80

Note that the three numbers in the columns on the right indicate displacement at the maximum, minimum and the difference between the maximum and minimum. The unit for them is [mm]. These numbers also are listed in Tables 5.2-2 – 5.2-4 .

Table 5.2-2 Deformations of a real RP assuming different inherent strains between the P and N sides

Model No.	Condition	Ux (radial)	Uy (thickness)	Uz (vertical)
Model 3(Ref. inboard)	After P side welding and restraint removal	-2.06/0.01 /2.07	-0.36/34.87 /35.23	0/0.39 /0.39
Model 4(Ref. outboard.)		-2.29/-0.03 2.32	-0.26/19.00 /19.26	0/0.37 0.37
Model 3(Ref. inboard)	After N side welding and restraint removal	-4.01/0.02 /4.03	-0.28/4.81 /5.09	-0.02/0.60 /3.50
Model 4(Ref. outboard.)		-4.28/0.02 /4.30	-0.28/2.967 /2.95	-0.03/0.65 /0.68

Table 5.2-3 Effect of welding thickness on RP displacement assuming the same inherent strains for the P and N sides

Model No./weld element length	Condition	Ux (radial)	Uy (thickness)	Uz (vertical)
Model 5 (Ref.) /Straight 3.5mm, Curved 2mm	After P side welding and restraint removal	-0.80/0.0 /0.80	-0.34/31.40 /31.74	0/0.31 /0.31
	After N side welding and restraint removal	-1.78/0.04 1.82	-0.36/0.27 0.63	0/0.50 0.50

Table 5.2-4 Effect of welding thickness on RP displacement assuming different inherent strains for the P and N sides

Model No./weld element length	Condition	Ux (radial)	Uy (thickness)	Uz (vertical)
Model 5 (Ref.) /Inboard 3.5mm, outboard 2mm	After P side welding and restraint removal	-0.80/0.0 /0.80	-0.34/31.40 /31.74	0/0.31 /0.31
	After N side welding and restraint removal	-1.52/0.02 /1.54	-0.29/4.18 4.47	0/0.46 0.46

Table 5.2-5 Effect of radial weld on RP displacement assuming the same inherent strains for the P and N sides

Model No./ weld	Condition	Ux (radial)	Uy (thickness)	Uz (vertical)
Model 6(Ref.) /14 weld lines in the radial direction	After P side welding and restraint removal	-0.30/0.17 /0.47	-0.25/5.14 /5.39	-0.09/0.26 /0.37
	After N side welding and restraint removal	-0.32/0.09 /0.41	-0.14/0.16 /0.30	-0.07/0.20 /0.27

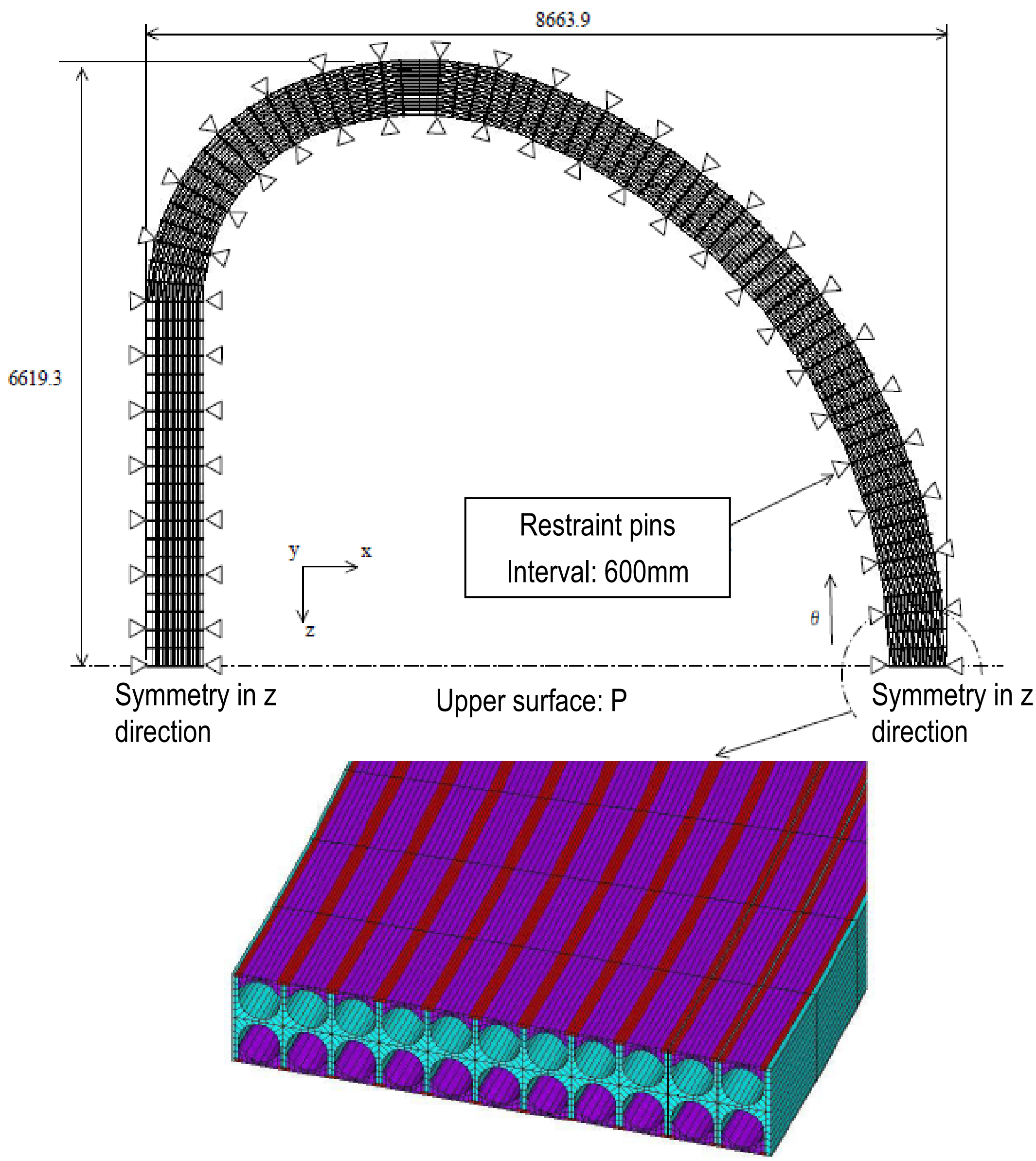

Fig. 5.1-1 Analytical model for welding between CPs and the RP teeth

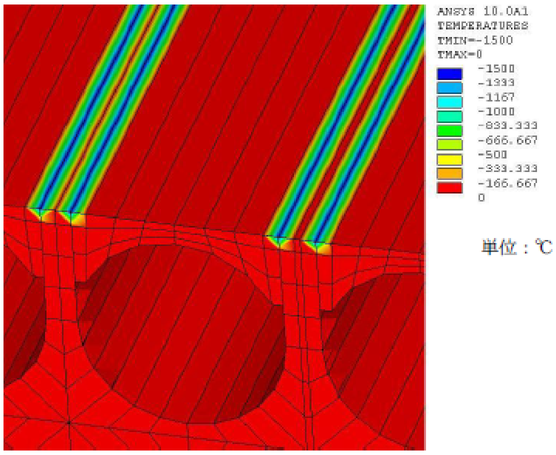

(a) Bird's-eye view

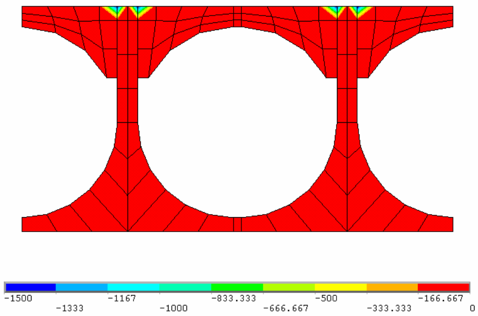

(b) Cross-sectional view

Fig.5.1-2 Detail of mesh

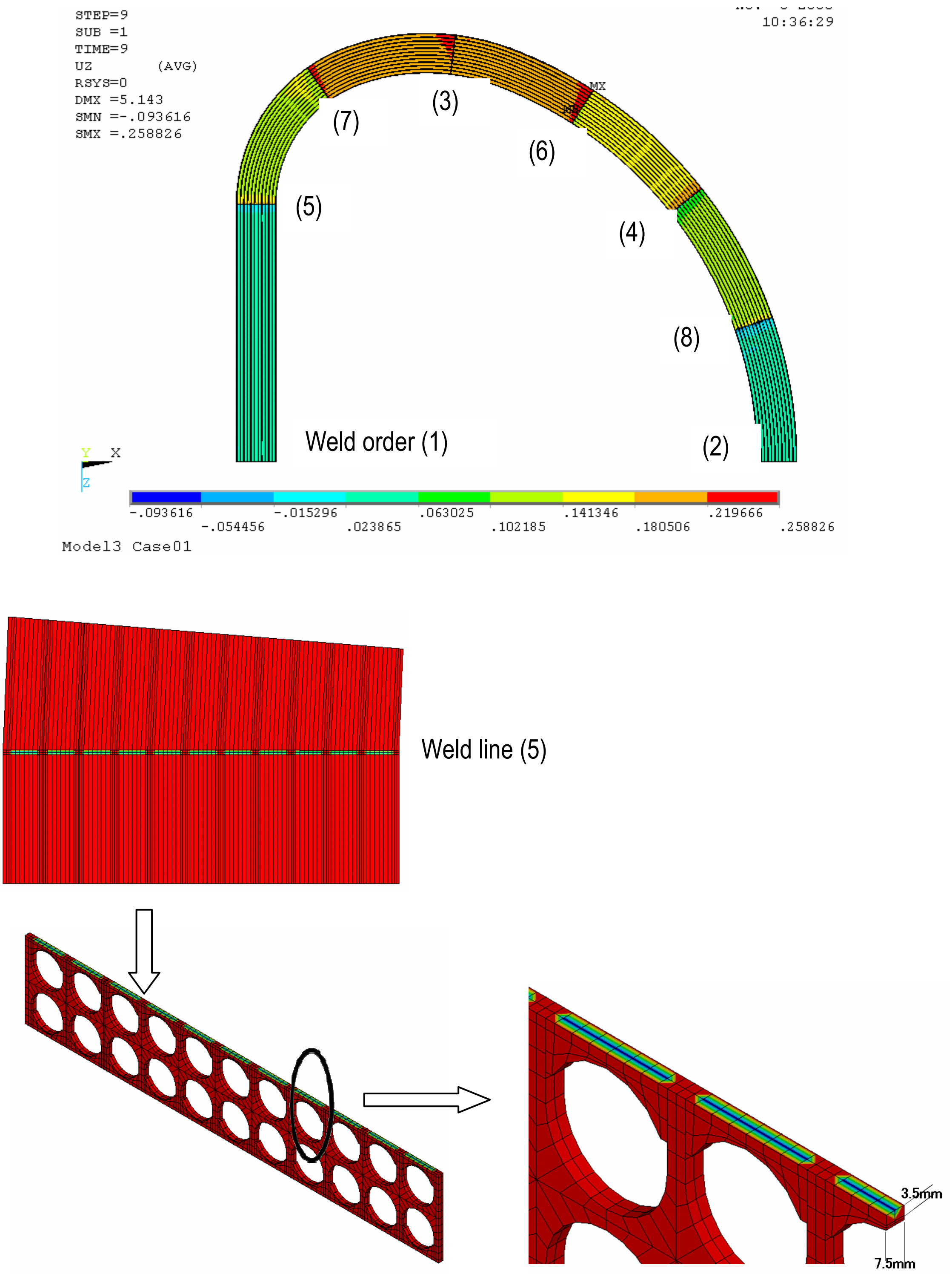

Fig. 5.1-3 Analytical model for welding between CPs

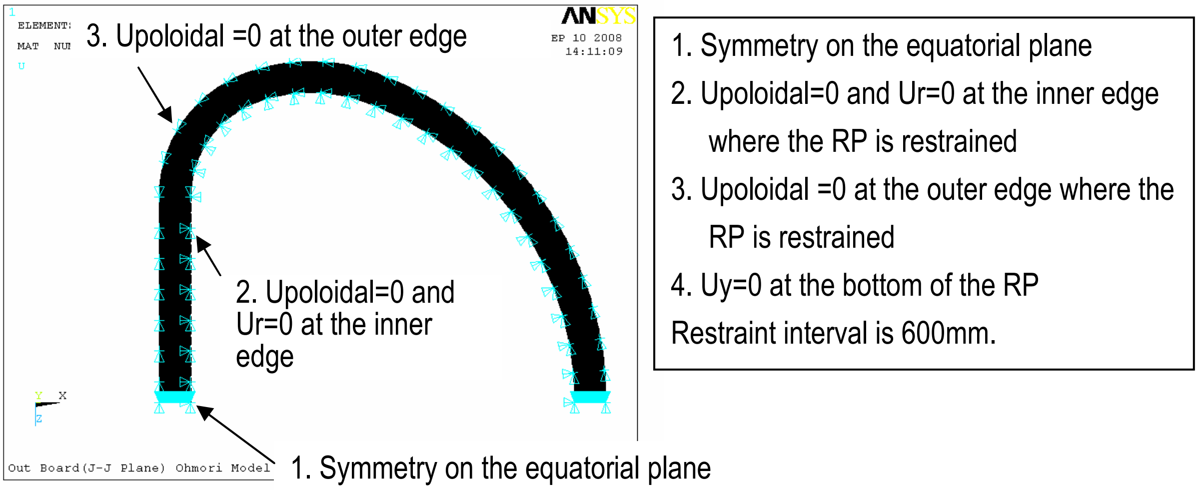

(a) Restraint during P side welding

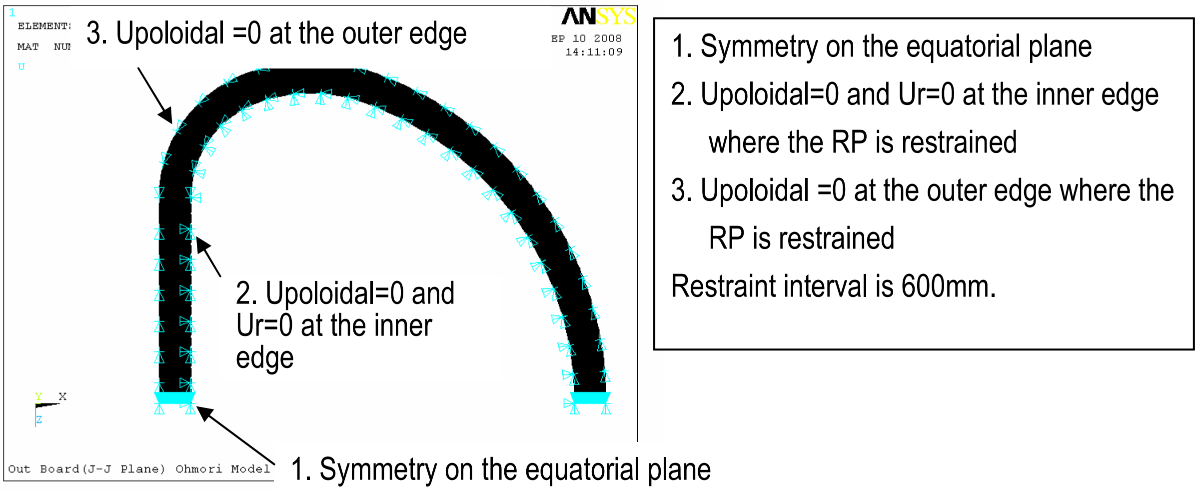

(b) Restraint during N side welding

Fig.5.1-4 Boundary conditions

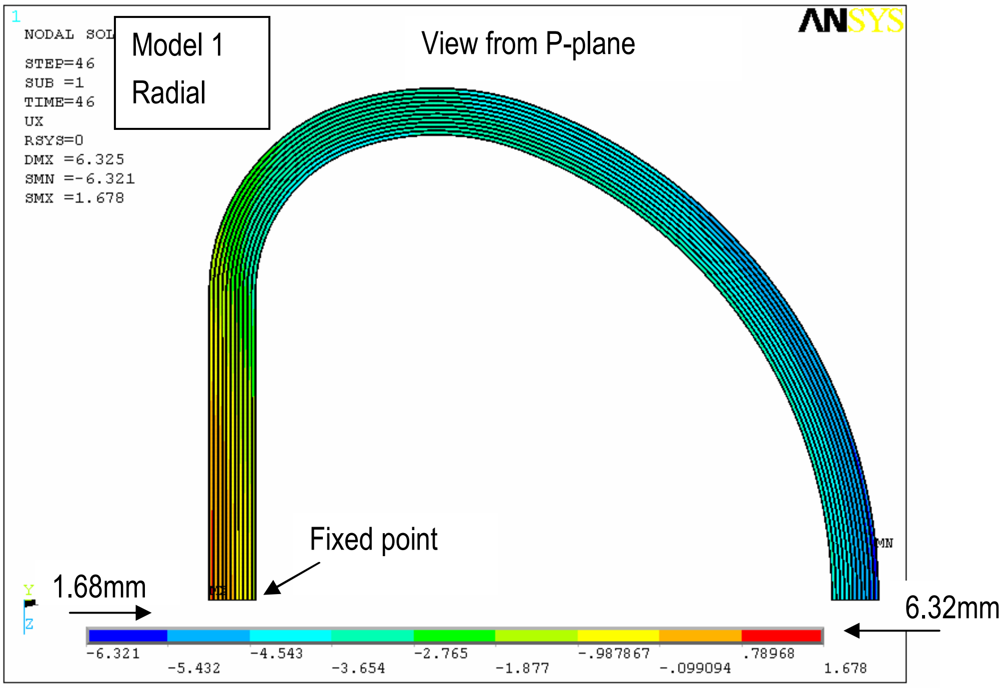

Fig.5.2-1 Deformation of the reference design in the radial direction after N side welding and constraint release assuming the same inherent strains

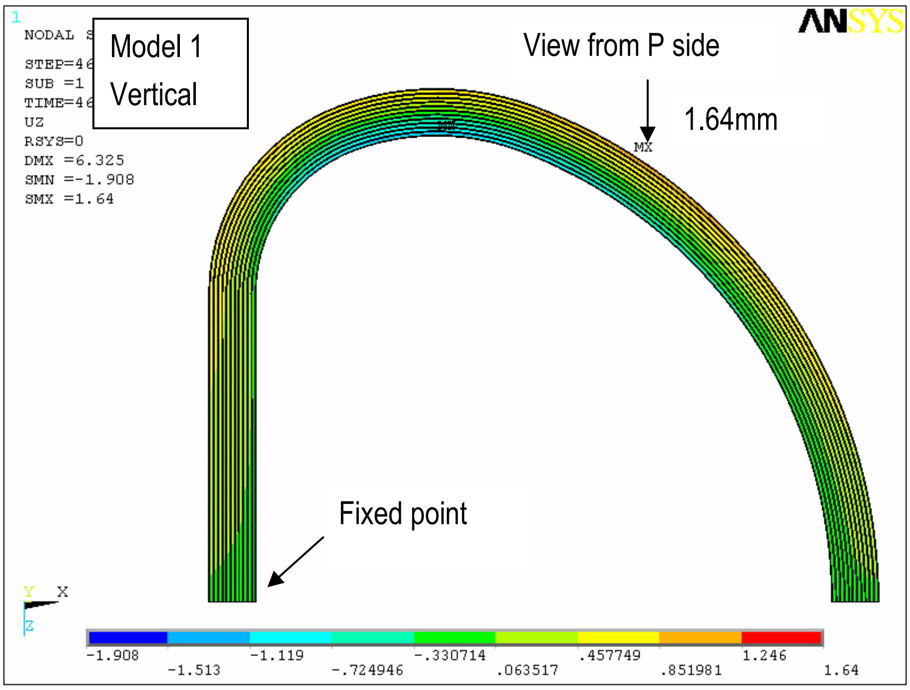

Fig.5.2-2 Deformation of the reference design in the vertical direction after N side welding and constraint release assuming the same inherent strains (Model1)

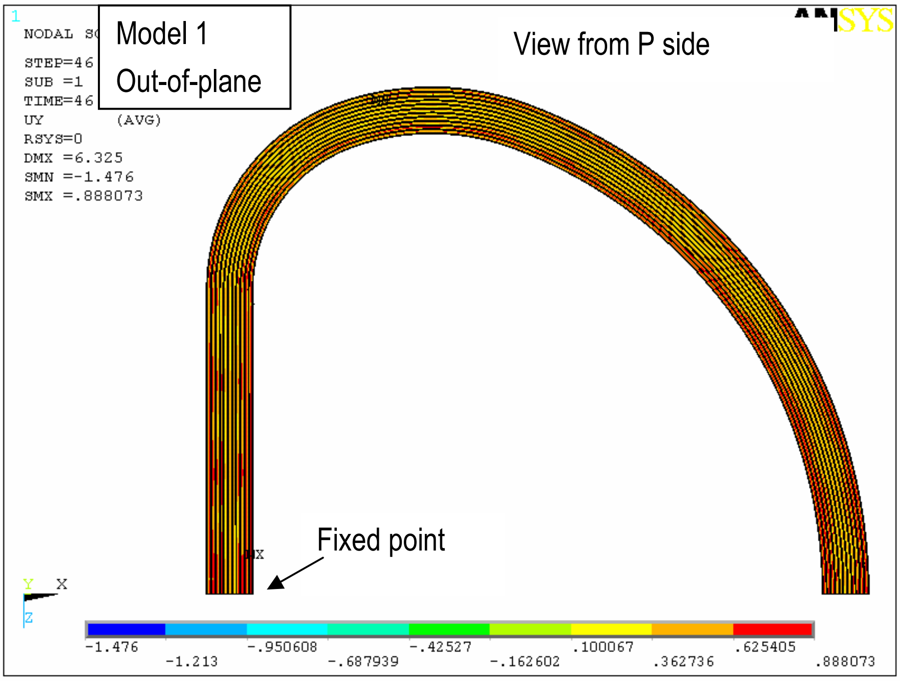

Fig.5.2-3 Deformation of the reference design in terms of thickness after N side welding and constraint release assuming the same inherent strains (Model1)

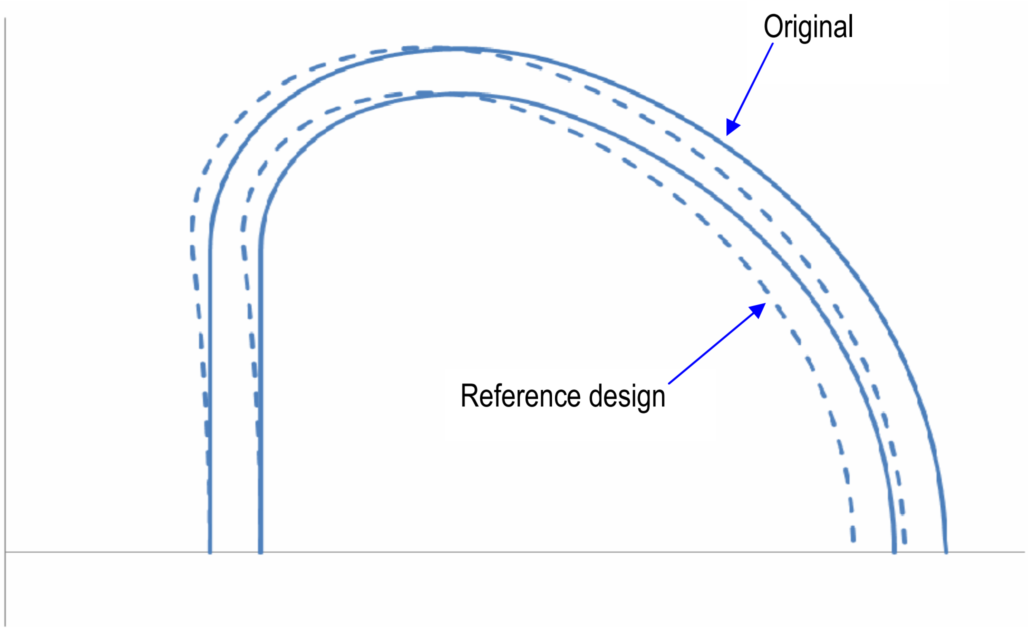

Fig. 5.2-4 In-plane deformation of the reference design after N side welding and restraint removal assuming the same inherent strains

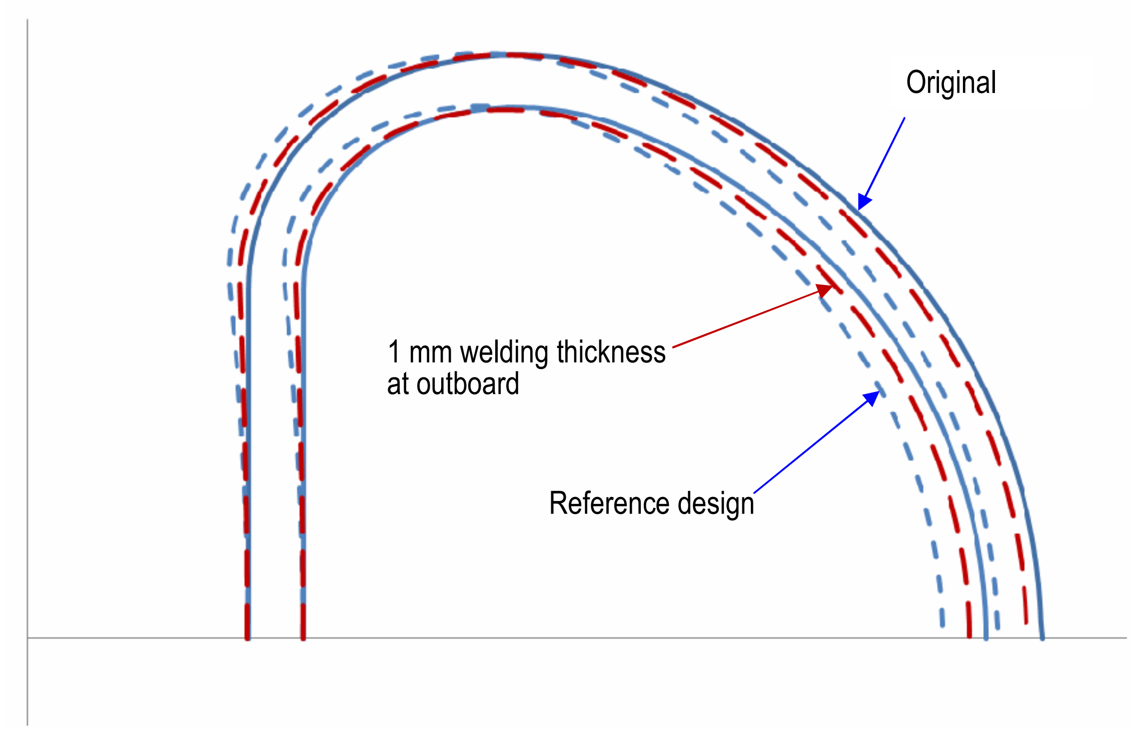

Fig. 5.2-5 In-plane deformation of the reference design and the model in which the welding thickness is reduced to 1 mm at the curved region after N side welding and restraint removal.

6. Alternative design for the RP and CP configuration

6.1 Details of an alternative design for the RP and CP configuration

The groove machining and manufacturing of CPs to meet the requirements of tight tolerances and adjusting the gaps between the CPs and the RP teeth seem time-consuming. We therefore are interested in developing an alternative design for the RP and CP to minimize the manufacturing load. One possible candidate is shown in **Fig. 6.1-1**. The RP is replaced by a thinner RP and the CP, by a spacer CP and a flat CP, as shown in Fig.6.1-1. Penetration laser-welding is used to affix the flat CP to the RP teeth, shown in **Fig. 6.1.2**. Spacer CPs are not continuously welded to the RP teeth but tack-welded.

The thickness of the flat CP would be 2.5mm. Since the welding thickness between CPs is around 2.5mm in the reference design, the stiffness of the alternative design in the Poloidal direction is anticipated to be the same as that of the reference design.

It is consequently expected that the alternative design will have the following advantages:

1) Tight tolerances for the CP and RP groove are not required.

   A high degree of accuracy in machining the RP groove and the CP is indispensable in the reference design to apply laser welding. In contrast, such tight tolerances are not necessary since the flat CP is welded to the RP teeth by penetration welding in the alternative design.

2) Easier assembly of CP into the RP groove

   The gap between the CP and the RP weld surfaces has be less than 0.2mm for laser welding. Precise gap adjustment is needed in the reference design. This seems difficult, especially due to the curvature of the CP. In contrast, such adjustments are not necessary in the alternative design.

3) Reduction of weld lines

   The number of weld lines per conductor may be reduced to half that of the reference design. A reduction in welding deformation also may be expected.

Comparisons between the reference and alternative designs are summarized in **Table 6.1-1**.

6.2 Welding deformation of the RP in the alternative design

Deformation due to CP welding in the alternative design is calculated so as to allow for comparison with that of the reference design. Welding conditions are the same as those of the reference design. The used mesh is shown in **Fig.6.2-1**. The cases of analysis are shown in **Table 6.2-1.** Note that only the outboard cross section is focused on in this study. The inherent strains are assumed to be the same and different between the P and N sides as stated in Models 7 and 8, respectively.

Calculated deformation listed in Models 7 and 8 is shown in **Tables 6.2-2** and **6.2-3**. Compared to Model 2 in **Table 5.2-1** and Model 4 in **Table 5.2-2**, all deformations in Models 7 and 8 are smaller than those of the reference design after N plane welding and restraint removal. Reducing the number of weld lines decreases welding deformation. The actual reduction in the distortion is minimal: 0.27 mm and 0.43mm for cases assuming identical and different inherent strains between the P and N sides. The distribution of deformation is shown in **Figs. 6.2-2 - 6.2-4**. The distribution is similar to those of the reference design.

Figure 6.2-5 shows in-plane deformation in the middle of the height of the RP for both the reference and alternative designs. The alternative design is less effective at reducing in-plane deformation more effective at reducing welding thickness at the outboard, compared to the reference design. However, since a reduction in welding at the outboard is also possible in the alternative design, deformation in its entirety could be smaller than those of the improved reference design, in which the welding thickness at the curved region is 1 mm.

Table 6.1-1 Comparison of fabrication between the reference and alternative designs

	Alternative Design	Reference Design
(1) Machining of RP and CP	Tight tolerances are not required	Precise machining is needed for the RP and CP grooves.
(2) Assembly of CP and RP	Tight tolerances are not required.	Bending and/or machining is required.
(3) Number of welding line	One weld line per conductor	Two weld lines per conductor
(4) Probability of stress concentration	None	Low

Table 6.2-1 Models for analyzing the alternative design of a real RP

Model No.	CP weld design	Inherent strains for P and N sides	Cross section of FEM model	No. of weld lines on one side	Depth of weld elements
Model 7	Alternative	Same strains	Outboard	Poloidal : 22	3.5mm
Model 8	Alternative	Different strains	Outboard	Poloidal : 22	3.5mm

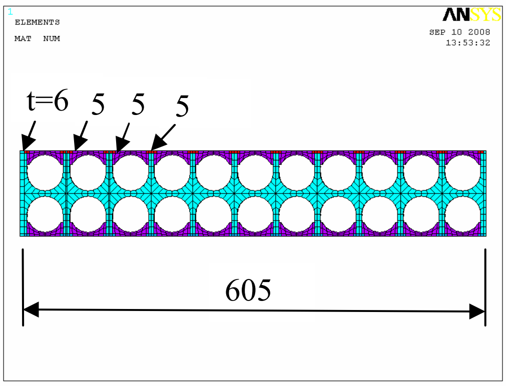

Outboard cross section

Table 6.2-2 Deformation of the alternative design of a real RP assuming the same inherent strains for the P and N sides

Model	Condition	Ux (radial)	Uy (thickness)	Uz (vertical)
Model 7 (Alter. outboard)	After P side welding and constraint removal	-1.49/0.06 /1.55	-0.76/16.36 /17.12	0/0.26 /0.26
Model 7 (Alter. outboard)	After N side welding and Constraint release	-3.10/0.15 /3.25	-0.65/0.64 /1.29	-0.05/0.49 /0.54

Note that the three numbers in the columns to the right indicate displacement at the maximum, minimum and the difference between the maximum and minimum. Unit are in [mm]. The same numbers are listed in Table 6.2-3 – 6.2-4.

Table 6.2-3 Deformations of a real RP assuming different inherent strains between the P and N sides

Model	Condition	Ux (radial)	Uy (thickness)	Uz (vertical)
Model 8 (Alter. outboard)	After P side welding and constraint release	-1.49/0.06 /1.55	-0.76/16.36 /17.12	0/0.26 /0.26
Model 8 (Alter. outboard)	After N side welding and Constraint release	-2.74/0.13 /2.87	-0.73/2.67 /3.40	0/0.46 /0.46

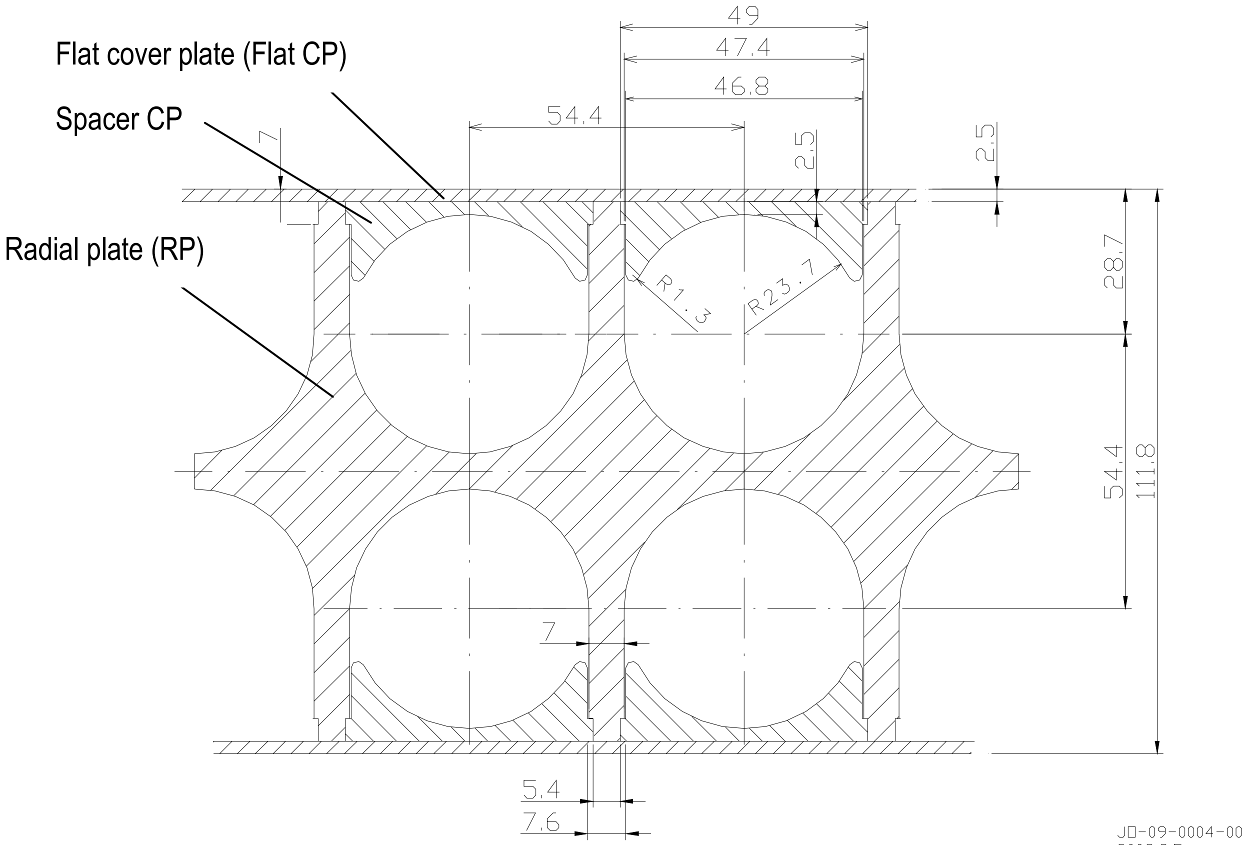

Fig. 6.1-1 Dimensions of an alternative design of an RP

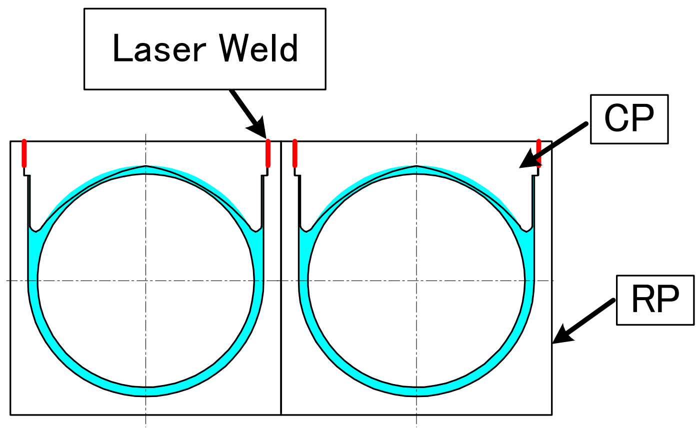

(a) CP weld lines for the reference design

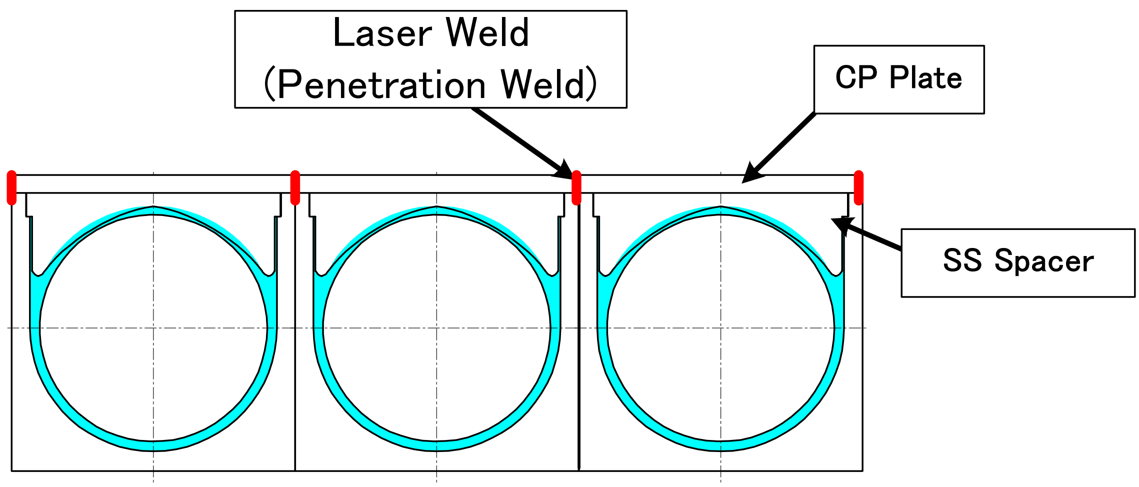

(b) CP welding in the alternative design

Fig. 6.1-2 Weld lines of the reference and alternative CP designs

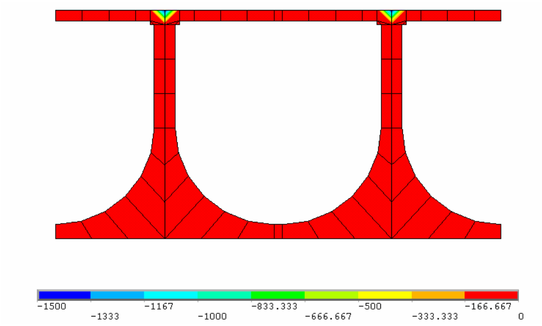

Fig. 6.2-1 Mesh pattern of the cross section of the alternative design

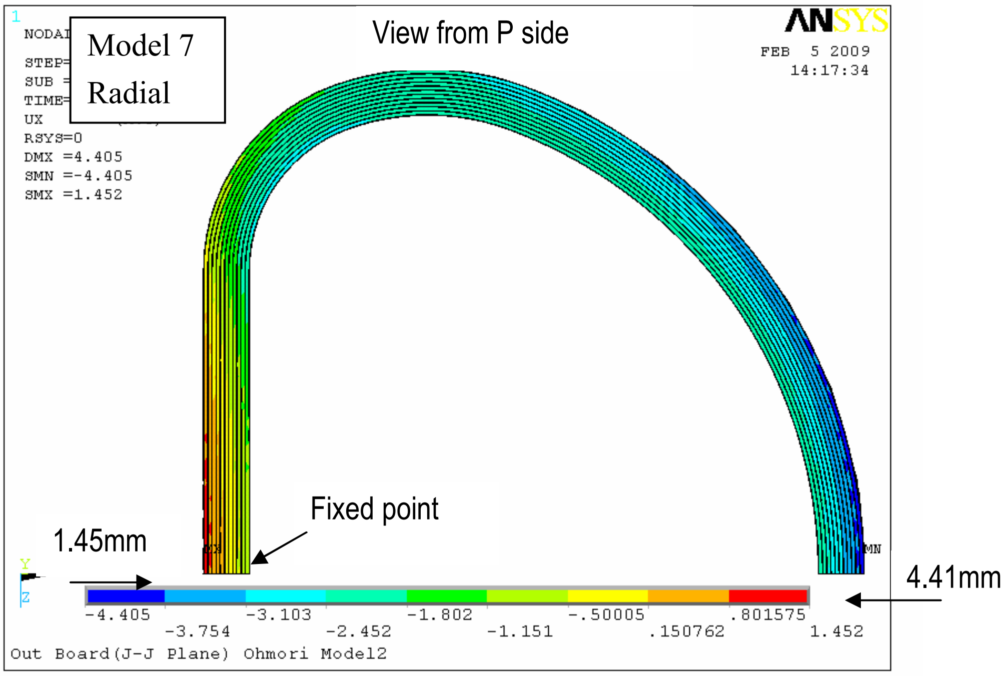

Fig.6.2-2 Deformation of the alternative design in the radial direction after N side welding and constraint release assuming the same inherent strains (Model7)

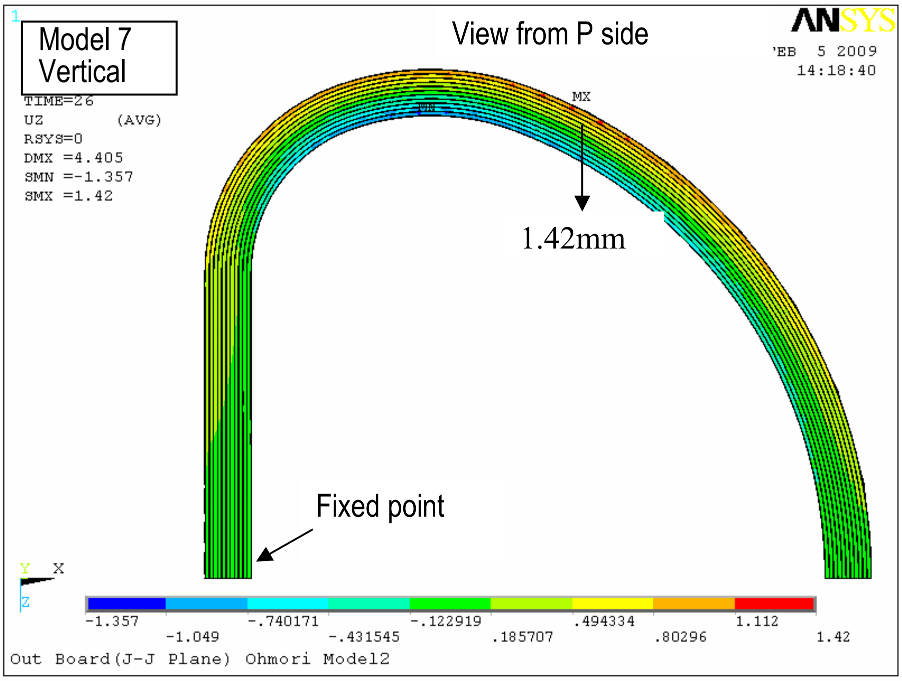

Fig.6.2-3 Deformation of the alternative design in the vertical direction after N side welding and constraint release assuming the same inherent strains (Model7)

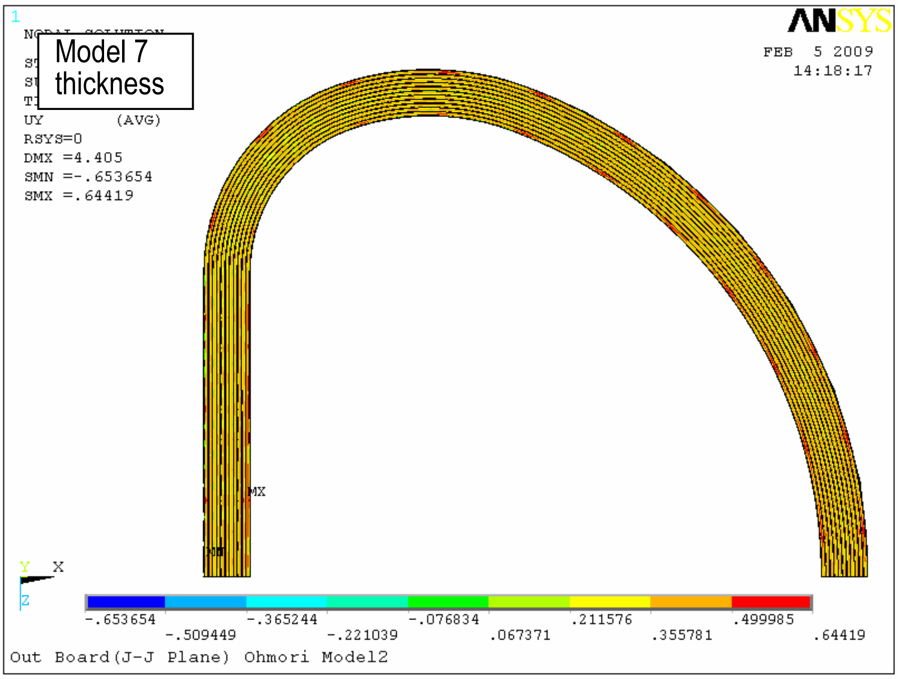

Fig.6.2-4 Deformation of the alternative design in the direction of thickness after N side welding and constraint release assuming the same inherent strains (Model7)

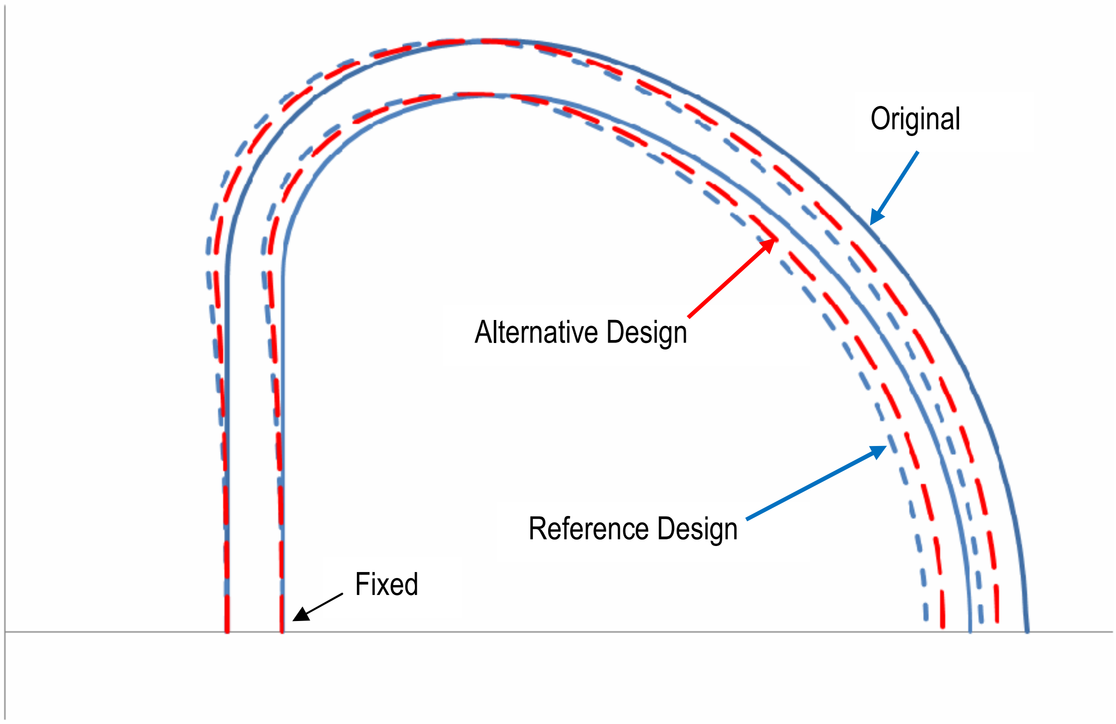

Fig.6.2-5 In-plane deformation of the reference and the alternative designs after N side welding and constraint release

7. Conclusions

In order to estimate the welding deformation of a full-scale RP, analysis using the inherent strain method is applied. The inherent strains are determined from test results of welding deformation. Therefore, CP welding tests were performed using a 1-m RP mock-up in the inboard curved region to determine the inherent strains. Deformation of the full scale RP is calculated using these inherent strains. In addition, an alternative design is proposed to simplify the fabrication procedure of the DP and to reduce deformations from welding. Major conclusions are as follows:

(1) CP welding tests using the RP mock-up

Out-of-plane deformation was measured to be less than 0.9 mm after CP welding on both sides. Note that the gap between the CP and the RP teeth before welding on the N side widened as a result of fixing the support beam along only the inner and outer surfaces. This increase in the gap enlarges the discrepancy in the estimate of inherent strains between the P and N sides. This discrepancy would probably be reduced if proper restraints were used.

(2) Analysis of welding deformation in a full-scale RP

The calculated out-of-plane distortion and in-plane deformation due to CP welding is 0.8 mm, which is within the target of 1 mm but marginal, and twice the requirement, respectively. Calculation results show that the main source of in-plane deformation is bending in the curved region, as is expected from a preliminary study. Therefore, a reduction in welding thickness at the curved region is a promising solution to reduce in-plane deformation. In fact, when the welding thickness is 1 mm at the curved region, the in-plane deformation is within the requirement. Thus, it is expected that reducing welding deformation can be used to satisfy the target by limiting welding thickness to 1 mm at the curved region.

(3) Alternative design

The alternative design proposed by the authors consists of a spacer CP which is thinner than that of the reference design, and a flat CP. The flat CP and the spacer CP are penetration-welded and tack-welded to the RP, respectively. Since the weld length is half of that of the reference design, welding deformation may be reduced. In addition, the alternative design has the advantages of having generous tolerances with regard to RP groove machining, shaping of the CP and gap adjustment between the CP and the RP.

Acknowledgement

The authors would like to thank to colleagues of ITER Superconducting Magnet Technology Group for many valuable discussions with them. The authors also wish to acknowledge Dr. Toshihide Tsunematsu and Dr. Ryuji Yoshino for their support.

References

[1] C. Sborchia, Y. Fu, R. Gallix, C. Jong, *et al.*, "Design and specification of the ITER TF coils," *IEEE Trans. ASC,* Vol. 18, 2008, pp.463-466.

[2] M. Mochizuki, M. Hayashi and T. Hattori, "Numerical analysis of welding residual stress and its verification using neutron diffraction measurement," *ASME Trans. J. Engineering Materials and Technology*, Vol. 122, No.1, 2000, pp.98-103.

[3] N. Koizumi, H. Nakajima, K. Matsui, T. Isono, *et al.*, "Results of R&D on ITER-TF winding critical issues," *IEEE Trans. ASC,* Vol. 18, 2008, pp.475-478.

国際単位系（SI）

表１．SI 基本単位

基本量	SI 基本単位	
	名称	記号
長さ	メートル	m
質量	キログラム	kg
時間	秒	s
電流	アンペア	A
熱力学温度	ケルビン	K
物質量	モル	mol
光度	カンデラ	cd

表２．基本単位を用いて表されるSI組立単位の例

組立量	SI 基本単位	
	名称	記号
面積	平方メートル	m^2
体積	立法メートル	m^3
速さ，速度	メートル毎秒	m/s
加速度	メートル毎秒毎秒	m/s^2
波数	毎メートル	m^{-1}
密度，質量密度	キログラム毎立方メートル	kg/m^3
面積密度	キログラム毎平方メートル	kg/m^2
比体積	立方メートル毎キログラム	m^3/kg
電流密度	アンペア毎平方メートル	A/m^2
磁界の強さ	アンペア毎メートル	A/m
量濃度(a)，濃度	モル毎立方メートル	mol/m^3
質量濃度	キログラム毎立法メートル	kg/m^3
輝度	カンデラ毎平方メートル	cd/m^2
屈折率(b)	（数字の）1	1
比透磁率(b)	（数字の）1	1

(a) 量濃度（amount concentration）は臨床化学の分野では物質濃度（substance concentration）ともよばれる。
(b) これらは無次元量あるいは次元１をもつ量であるが、そのことを表す単位記号である数字の１は通常は表記しない。

表３．固有の名称と記号で表されるSI組立単位

組立量	SI 組立単位			
	名称	記号	他のSI単位による表し方	SI基本単位による表し方
平面角	ラジアン(b)	rad	1(b)	m/m
立体角	ステラジアン(b)	sr(c)	1(b)	m^2/m^2
周波数	ヘルツ(d)	Hz		s^{-1}
力	ニュートン	N		$m\ kg\ s^{-2}$
圧力，応力	パスカル	Pa	N/m^2	$m^{-1}\ kg\ s^{-2}$
エネルギー，仕事，熱量	ジュール	J	N m	$m^2\ kg\ s^{-2}$
仕事率，工率，放射束	ワット	W	J/s	$m^2\ kg\ s^{-3}$
電荷，電気量	クーロン	C		s A
電位差（電圧），起電力	ボルト	V	W/A	$m^2\ kg\ s^{-3}\ A^{-1}$
静電容量	ファラド	F	C/V	$m^{-2}\ kg^{-1}\ s^4\ A^2$
電気抵抗	オーム	Ω	V/A	$m^2\ kg\ s^{-3}\ A^{-2}$
コンダクタンス	ジーメンス	S	A/V	$m^{-2}\ kg^{-1}\ s^3\ A^2$
磁束	ウエーバ	Wb	Vs	$m^2\ kg\ s^{-2}\ A^{-1}$
磁束密度	テスラ	T	Wb/m^2	$kg\ s^{-2}\ A^{-1}$
インダクタンス	ヘンリー	H	Wb/A	$m^2\ kg\ s^{-2}\ A^{-2}$
セルシウス温度	セルシウス度(e)	℃		K
光束	ルーメン	lm	cd sr(c)	cd
照度	ルクス	lx	lm/m^2	$m^{-2}\ cd$
放射性核種の放射能(f)	ベクレル(d)	Bq		s^{-1}
吸収線量, 比エネルギー分与, カーマ	グレイ	Gy	J/kg	$m^2\ s^{-2}$
線量当量, 周辺線量当量, 方向性線量当量, 個人線量当量	シーベルト(g)	Sv	J/kg	$m^2\ s^{-2}$
酸素活性	カタール	kat		$s^{-1}\ mol$

(a)SI接頭語は固有の名称と記号を持つ組立単位と組み合わせても使用できる。しかし接頭語を付した単位はもはやコヒーレントではない。
(b)ラジアンとステラジアンは数字の１に対する単位の特別な名称で、量についての情報をつたえるために使われる。実際には、使用する時には記号rad及びsrが用いられるが、習慣として組立単位としての記号である数字の１は明示されない。
(c)測光学ではステラジアンという名称と記号srを単位の表し方の中に、そのまま維持している。
(d)ヘルツは周期現象についてのみ、ベクレルは放射性核種の統計的過程についてのみ使用される。
(e)セルシウス度はケルビンの特別な名称で、セルシウス温度を表すために使用される。セルシウス度とケルビンの単位の大きさは同一である。したがって、温度差や温度間隔を表す数値はどちらの単位で表しても同じである。
(f)放射性核種の放射能（activity referred to a radionuclide）は、しばしば誤った用語で"radioactivity"と記される。
(g)単位シーベルト（PV,2002,70,205）についてはCIPM勧告2（CI-2002）を参照。

表４．単位の中に固有の名称と記号を含むSI組立単位の例

組立量	SI 組立単位		
	名称	記号	SI 基本単位による表し方
粘度	パスカル秒	Pa s	$m^{-1}\ kg\ s^{-1}$
力のモーメント	ニュートンメートル	N m	$m^2\ kg\ s^{-2}$
表面張力	ニュートン毎メートル	N/m	$kg\ s^{-2}$
角速度	ラジアン毎秒	rad/s	$m\ m^{-1}\ s^{-1}=s^{-1}$
角加速度	ラジアン毎秒毎秒	rad/s^2	$m\ m^{-1}\ s^{-2}=s^{-2}$
熱流密度，放射照度	ワット毎平方メートル	W/m^2	$kg\ s^{-3}$
熱容量，エントロピー	ジュール毎ケルビン	J/K	$m^2\ kg\ s^{-2}\ K^{-1}$
比熱容量，比エントロピー	ジュール毎キログラム毎ケルビン	J/(kg K)	$m^2\ s^{-2}\ K^{-1}$
比エネルギー	ジュール毎キログラム	J/kg	$m^2\ s^{-2}$
熱伝導率	ワット毎メートル毎ケルビン	W/(m K)	$m\ kg\ s^{-3}\ K^{-1}$
体積エネルギー	ジュール毎立方メートル	J/m^3	$m^{-1}\ kg\ s^{-2}$
電界の強さ	ボルト毎メートル	V/m	$m\ kg\ s^{-3}\ A^{-1}$
電荷密度	クーロン毎立方メートル	C/m^3	$m^{-3}\ sA$
表面電荷	クーロン毎平方メートル	C/m^2	$m^{-2}\ sA$
電束密度，電気変位	クーロン毎平方メートル	C/m^2	$m^{-2}\ sA$
誘電率	ファラド毎メートル	F/m	$m^{-3}\ kg^{-1}\ s^4\ A^2$
透磁率	ヘンリー毎メートル	H/m	$m\ kg\ s^{-2}\ A^{-2}$
モルエネルギー	ジュール毎モル	J/mol	$m^2\ kg\ s^{-2}\ mol^{-1}$
モルエントロピー, モル熱容量	ジュール毎モル毎ケルビン	J/(mol K)	$m^2\ kg\ s^{-2}\ K^{-1}\ mol^{-1}$
照射線量（Ｘ線及びγ線）	クーロン毎キログラム	C/kg	$kg^{-1}\ sA$
吸収線量率	グレイ毎秒	Gy/s	$m^2\ s^{-3}$
放射強度	ワット毎ステラジアン	W/sr	$m^4\ m^{-2}\ kg\ s^{-3}=m^2\ kg\ s^{-3}$
放射輝度	ワット毎平方メートル毎ステラジアン	$W/(m^2\ sr)$	$m^2\ m^{-2}\ kg\ s^{-3}=kg\ s^{-3}$
酵素活性濃度	カタール毎立方メートル	kat/m^3	$m^{-3}\ s^{-1}\ mol$

表５．SI 接頭語

乗数	接頭語	記号	乗数	接頭語	記号
10^{24}	ヨタ	Y	10^{-1}	デシ	d
10^{21}	ゼタ	Z	10^{-2}	センチ	c
10^{18}	エクサ	E	10^{-3}	ミリ	m
10^{15}	ペタ	P	10^{-6}	マイクロ	µ
10^{12}	テラ	T	10^{-9}	ナノ	n
10^{9}	ギガ	G	10^{-12}	ピコ	p
10^{6}	メガ	M	10^{-15}	フェムト	f
10^{3}	キロ	k	10^{-18}	アト	a
10^{2}	ヘクト	h	10^{-21}	ゼプト	z
10^{1}	デカ	da	10^{-24}	ヨクト	y

表６．SIに属さないが、SIと併用される単位

名称	記号	SI 単位による値
分	min	1 min=60s
時	h	1h =60 min=3600 s
日	d	1 d=24 h=86 400 s
度	°	1°=(π/180) rad
分	’	1’=(1/60)°=(π/10800) rad
秒	”	1”=(1/60)’=(π/648000) rad
ヘクタール	ha	$1ha=1hm^2=10^4m^2$
リットル	L，l	$1L=1l=1dm^3=10^3cm^3=10^{-3}m^3$
トン	t	$1t=10^3$ kg

表７．SIに属さないが、SIと併用される単位で、SI単位で表される数値が実験的に得られるもの

名称	記号	SI 単位で表される数値
電子ボルト	eV	$1eV=1.602\ 176\ 53(14)\times10^{-19}J$
ダルトン	Da	$1Da=1.660\ 538\ 86(28)\times10^{-27}kg$
統一原子質量単位	u	1u=1 Da
天文単位	ua	$1ua=1.495\ 978\ 706\ 91(6)\times10^{11}m$

表８．SIに属さないが、SIと併用されるその他の単位

名称	記号	SI 単位で表される数値
バール	bar	$1\ bar=0.1MPa=100kPa=10^5Pa$
水銀柱ミリメートル	mmHg	1mmHg=133.322Pa
オングストローム	Å	$1\ Å=0.1nm=100pm=10^{-10}m$
海里	M	1 M=1852m
バーン	b	$1\ b=100fm^2=(10^{-12}cm)2=10^{-28}m^2$
ノット	kn	1 kn=(1852/3600)m/s
ネーパ	Np	SI単位との数値的な関係は、対数量の定義に依存。
ベル	B	
デジベル	dB	

表９．固有の名称をもつCGS組立単位

名称	記号	SI 単位で表される数値
エルグ	erg	$1\ erg=10^{-7}\ J$
ダイン	dyn	$1\ dyn=10^{-5}N$
ポアズ	P	$1\ P=1\ dyn\ s\ cm^{-2}=0.1Pa\ s$
ストークス	St	$1\ St=1cm^2\ s^{-1}=10^{-4}m^2\ s^{-1}$
スチルブ	sb	$1\ sb=1cd\ cm^{-2}=10^4cd\ m^{-2}$
フォト	ph	$1\ ph=1cd\ sr\ cm^{-2}\ 10^4lx$
ガル	Gal	$1\ Gal=1cm\ s^{-2}=10^{-2}ms^{-2}$
マクスウェル	Mx	$1\ Mx = 1G\ cm^2=10^{-8}Wb$
ガウス	G	$1\ G=1Mx\ cm^{-2}=10^{-4}T$
エルステッド(c)	Oe	$1\ Oe \triangleq (10^3/4\pi)A\ m^{-1}$

(c) ３元系のCGS単位系とSIでは直接比較できないため、等号「 ≙ 」は対応関係を示すものである。

表10．SIに属さないその他の単位の例

名称	記号	SI 単位で表される数値
キュリー	Ci	$1\ Ci=3.7\times10^{10}Bq$
レントゲン	R	$1\ R = 2.58\times10^{-4}C/kg$
ラド	rad	$1\ rad=1cGy=10^{-2}Gy$
レム	rem	$1\ rem=1\ cSv=10^{-2}Sv$
ガンマ	γ	1γ=1 nT=10-9T
フェルミ		1フェルミ=1 fm=10-15m
メートル系カラット		1メートル系カラット = 200 mg = 2×10-4kg
トル	Torr	1 Torr = (101 325/760) Pa
標準大気圧	atm	1 atm = 101 325 Pa
カロリー	cal	1cal=4.1858J（「15℃」カロリー），4.1868J（「IT」カロリー）4.184J（「熱化学」カロリー）
ミクロン	µ	$1\ \mu=1\mu m=10^{-6}m$

（第8版，2006年改訂）